Paul, V.J., Yeddanapalli, L.M., 1956. On the olefinic nature of anacardic acid from Indian cashew nut shell liquid. J. Am. Chem. Soc. 78, 5675–5678.

Petkovich, M., Brand, N.J., Krust, A., Chambon, P., 1987. A human retinoic acid receptor which belongs to the family of nuclear receptors. Nature 330, 444–450.

Sherf, B.A., Navarro, S.L., Hannah, R.R., Wood, K.V., 1996. Dual-luciferase™ reporter assay: an advanced co-reporter technology integrating firefly and *Renilla* luciferase assays. Promega Notes 57, 2.

Sinal, C.J., Tohkin, M., Miyata, M., Ward, J.M., Lambert, G., Gonzalez, F.J., 2000. Targeted disruption of the nuclear receptor FXR/BAR impairs bile acid and lipid homeostasis. Cell 102, 731–744.

Su, Z.-Z., Lin, J., Grunberger, D., Fisher, P.B., 1994. Growth suppression and toxicity induced by caffeic acid phenethyl ester (CAPE) in type 5 adenovirus-transformed rat embryo cells correlate directly with transformation progression. Cancer Res. 54, 1865–1870.

Sugiyama, K., Kawagishi, H., Tanaka, A., Saeki, S., Yoshida, S., Sakamoto, H., Ishiguro, Y., 1992. Isolation of plasma cholesterol-lowering components from Ningyotake (*Polyporus confluens*) mushroom. J. Nutr. Sci. Vitaminol. 38, 335–342.

Sugiyama, K., Tanaka, A., Kawagishi, H., Ojima, F., Sakamoto, H., Ishiguro, Y., 1994. Hypocholesterolemic action of dietary grifolin on rats fed with a high-cholesterol diet. Biosci. Biotechnol. Biochem. 58, 211–212.

Toyota, M., Asakawa, Y., 1988. Sesquiterpenoids from the liverwort *Bazzania fauriana*. Phytochemistry 27, 2155–2159.

Urizar, N.L., Dowhan, D.H., Moore, D.D., 2000. The farnesoid X-activated receptor mediates bile acid activation of phospholipid transfer protein gene expression. J. Biol. Chem. 275, 39313–39317.

Wang, H., Chen, J., Hollister, K., Sowers, L.C., Forman, B.M., 1999. Endogenous bile acids are ligands for the nuclear receptor FXR/BAR. Mol. Cell 3, 543–553.

Watabe, M., Hishikawa, K., Takayanagi, A., Shimizu, N., Nakaki, T., 2004. Caffeic acid phenethyl ester induces apoptosis by inhibition of NFκB and activation of Fas in human breast cancer MCF-7 cells. J. Biol. Chem. 279, 6017–6026.

0026-895X/06/7001-319–328$20.00
MOLECULAR PHARMACOLOGY
Copyright © 2006 The American Society for Pharmacology and Experimental Therapeutics
Mol Pharmacol 70:319–328, 2006

Vol. 70, No. 1
20511/3124430
Printed in U.S.A.

Retinoic Acids Increase $P2X_2$ Receptor Expression through the 5′-Flanking Region of *P2rx2* Gene in Rat Phaeochromocytoma PC-12 Cells

Hidetoshi Tozaki-Saitoh, Schuichi Koizumi, Yoji Sato, Makoto Tsuda, Taku Nagao, and Kazuhide Inoue

Divisions of Pharmacology (H.T.-S., S.K.) and Cellular and Gene Therapy Products (Y.S.), National Institute of Health Sciences, Tokyo, Japan; National Institute of Health Sciences, Tokyo, Japan (T.N.); and Department of Molecular and System Pharmacology, Graduate School of Pharmaceutical Sciences, Kyushu University, Fukuoka, Japan (H.T.-S., M.T., K.I.)

Received November 1, 2005; accepted April 25, 2006

ABSTRACT

The $P2X_2$ receptor is a subtype of ionotropic ATP receptor and plays a significant role in regulating fast synaptic transmission in the nervous system. Because the expression level of the $P2X_2$ receptor is known to determine its channel properties and functional interactions with other neurotransmitter channels, elucidating the mechanisms underlying the regulation of $P2X_2$ receptor expression in neuronal cells is important. Here, we identified three motifs that correspond to the retinoic acid response element in the 5′-flanking region of the rat $P2X_2$ gene. In rat pheochromocytoma PC-12 cells, treatment with 9-*cis*-retinoic acid as well as all-*trans*-retinoic acid significantly increased the mRNA and protein level of $P2X_2$ receptor. In addition, in PC-12 cells transiently transfected with a luciferase reporter gene driven by the promoter region of the rat $P2X_2$ gene, both 9-*cis*-retinoic acid and all-*trans*-retinoic acid increased the luciferase activity, whereas their effects were diminished by truncation of the retinoic acid response elements in the promoter. Furthermore, 9-*cis*-retinoic acid enhanced the ATP-evoked whole cell currents and intracellular Ca^{2+}- and ATP-evoked dopamine release, indicating the up-regulation of functional $P2X_2$ receptors on the plasma membrane. These results provide the molecular mechanism underlying the transcriptional regulation of $P2X_2$ receptors and suggest that retinoid is an important factor in regulating $P2X_2$ receptors in the nervous system.

P2X receptors, of which seven subtypes ($P2X_1$–$P2X_7$) have so far been cloned, are a family of ligand-gated cation channels activated by extracellular ATP and are widely expressed in the peripheral and central nervous system (North, 2002; Illes and Alexandre Ribeiro, 2004). A growing body of evidence indicates that P2X receptors expressed in neurons play important roles in mediating (Galligan and Bertrand, 1994), facilitating presynaptically (Khakh et al., 2003; Shigetomi and Kato, 2004), and modulating postsynaptically fast excitatory and inhibitory synaptic transmission (Wang et al., 2004). It remains unclear which P2X receptor subtypes are the main targets for ATP at synapses, but several lines of evidence have suggested the $P2X_2$ receptor as a candidate. In several regions of the nervous system, neurons express functional $P2X_2$ receptors (North, 2002; Illes and Alexandre Ribeiro, 2004) as well as both the mRNA and protein of $P2X_2$ receptors (Kanjhan et al., 1999). An electron microscopic study has shown that $P2X_2$ receptors are localized at the postsynaptic membrane in the cerebellum and the CA1 region of the hippocampus (Rubio and Soto, 2001). In addition, it has been reported that $P2X_2$ receptors are abundant in the biochemically fractionated presynaptic active zone in the hippocampus (Rodrigues et al., 2005). A recent study has shown that ATP facilitates excitatory glutamate transmission onto stratum radiatum interneurons, a population of the ATP-

This work was partly supported by The National Institute of Biomedical Innovation (Medical Frontier Project; MF-16), The Health Science Foundation in Japan, and a grant-in-aid for scientific research from the Ministry of Education, Science, Sports and Culture.

Article, publication date, and citation information can be found at http://molpharm.aspetjournals.org.

doi:10.1124/mol.105.020511.

ABBREVIATIONS: RARE, retinoic acid response element; RAR, retinoic acid receptor; RXR, retinoid X receptor; DA, dopamine; VDCC, voltage-dependent calcium channel; RA, retinoic acid; RT-PCR, reverse transcriptase polymerase chain reaction; bp, base pair(s); PCR, polymerase chain reaction; TESS, transcription element search system; RACE, rapid amplification of cDNA ends; $P2X_2R$, $P2X_2$ receptor; GAPDH, glyceraldehyde-3-phosphate dehydrogenase; GFP, green fluorescent protein; BSS, balanced salt solution; PCA, perchloric acid; AP, adaptor protein; atRA, all-*trans*-retinoic acid; PPADS, pyridoxal phosphate-6-azophenyl-2′4′-disulfonic acid; U-73122, 1-[6-[[17β-methoxyestra-1,3,5(10)-trien-17-yl]amino]hexyl]-1*H*-pyrrole-2,5-dione; DR, direct repeat; ANOVA, analysis of variance.

responding neurons that is markedly reduced in hippocampus slices from $P2X_2$-deficient mice (Khakh et al., 2003). These results indicate that in several regions $P2X_2$ receptors localized at pre- and/or postsynapses regulate fast synaptic transmission. Furthermore, $P2X_2$ receptors are associated directly with other neurotransmitter channels such as nicotinic acetylcholine receptors, 5-hydroxytryptamine receptors or $GABA_A$ receptors, and activation of both receptors produces nonadditive cross-inhibitory responses (Khakh et al., 2000; Boue-Grabot et al., 2003). It is noteworthy that the functional interaction of $P2X_2$ receptors with other channels is decreased at lower densities of channel expression (Khakh et al., 2000), suggesting that their expression levels affect cellular events resulting from activation of $P2X_2$ receptors at synapses. In addition, the expression level of $P2X_2$ receptors also changes their channel properties (Fujiwara and Kubo, 2004). Moreover, an increase in the expression of $P2X_2$ receptors in neuronal cells has been implicated in the development of several pathological states such as brain ischemia and chronic pain (Xu and Huang, 2002; Cavaliere et al., 2003). Therefore, to understand the physiological and pathological roles of $P2X_2$ receptors in the functioning of the nervous system, it is of particular importance to determine how the expression of $P2X_2$ receptors is regulated in neuronal cells.

In the present study, we cloned the 5′-flanking region of the rat $P2X_2$ gene (*P2rx2*) and identified three sites corresponding to a motif of retinoic acid response element (RARE). RARE is a binding site of nuclear receptors, including retinoic acid receptor (RAR) and retinoid X receptor (RXR), and is required for the gene expression induced by retinoids (Chambon, 1996). We further found that retinoids increase both the mRNA and protein expression of the $P2X_2$ receptor and enhance release of the neurotransmitter dopamine (DA) evoked by ATP through activating $P2X_2$ receptors from rat pheochromocytoma PC-12 cells, a neuronal model (Shafer and Atchison, 1991). Therefore, these results suggest that retinoids are regulators of the expression of $P2X_2$ receptors in neuronal cells in the nervous system.

Materials and Methods

PC-12 Cells. PC-12 cells (passage 55–70) were cultured according to Inoue and Kenimer (1988), and undifferentiated cells were used. Cells were cultured in Dulbecco's modified eagle's medium supplemented with 7.5% fetal bovine serum, 7.5% horse serum, and 4 mM L-glutamine. For reverse transcription-polymerase chain reaction (RT-PCR) and Western blot experiments, cells were plated on 60-mm collagen (Virtogen-100)-coated dishes for 2 days. For whole cell patch-clamp recording and intracellular calcium imaging, cells were plated on collagen-coated coverslips placed on the bottom of 35-mm polystyrene dishes. For the measurement of DA release, cells were plated on collagen-coated 35-mm polystyrene dishes.

Cloning of the $P2X_2$ Upstream Region. Sequences for the 5′-flanking region of *P2rx2* were obtained from National Center for Biotechnology Information Rat Genome Resources. The genomic 2.5-kb upstream sequence of the putative Wistar rat *P2rx2* transcription starting site was targeted as $P2X_2$ mRNA (GenBank accession number NM_053656) upstream sequence. The following primers were designed for amplification of the 5′-flanking region of *P2rx2*: forward primer, GAACCTCGAGTGAGCCACAACCAGAACACT; reverse primer, GACAAGATCTATGGCCCAAGGAGCTCGGT. Genomic DNA extracted from the tail of a female Wistar rat was used for the polymerase chain reaction. Four individual reactions were carried out, and amplicons were inserted in a pGEM-T vector (Promega, Madison, WI) for sequencing. Each insert was sequenced, and the exact sequence was estimated by comparing the four sequences. The relative location of the cloned sequence is confirmed to be just upstream of the first exon of *P2rx2* without any intervening inserts. Using primers specific to the third exon of *P2rx2* and −164 position of the cloned sequence, approximately 750-bp single-band amplification was obtained by PCR. This amplicon included the sequence comprising the 5′ site of $P2X_2$ mRNA (RefSeq sequence NM_053656) exactly as published, and the sequence was determined to be the 5′-flanking region without any additional intervening sequence. The sequence data from the 5′-flanking region of *P2rx2* has been deposited in GenBank with the accession number AY749416. Putative sites for the transcription element were analyzed using Transcription Element Search System (TESS) site (http://www.cbil.upenn.edu/tess).

"Oligo-Capping" 5′ Rapid Amplification of cDNA Ends of $P2X_2$ mRNA. Modified rapid amplification of 5′ cDNA ends (5′ RACE) was performed according to oligo-capping method developed by Maruyama and Sugano (1994). Total RNA (5 μg) extracted from PC-12 cells was treated with 1 unit of bacterial alkaline phosphatase (Takara, Kyoto, Japan) in supplied buffer with 100 units of RNase inhibitor (Toyobo, Osaka, Japan) at 37°C for 30 min to hydrolyze the phosphate of truncated mRNA 5′ ends. After extraction with phenol/chloroform (1:1) twice, chloroform once, and ethanol precipitation, tobacco acid pyrophosphatase (20 units; Wako Pure Chemicals, Osaka, Japan) was reacted (37°C; 15 min) in kit supplied buffer with RNase inhibitor to remove the cap structure of complete mRNAs. After phenol/chloroform extraction and ethanol precipitation, ligation reaction was carried with T4 RNA ligase (Takara) and 0.5 μg of 5′-adapter RNA oligonucleotide to obtain the oligonucleotide composed by mRNAs attached with 5′-adapter RNA oligonucleotide at 5′ ends that originally had the cap structure. After unligated 5′-adapter oligonucleotide was removed by repeating ethanol precipitation with high salt concentration, reverse transcription reaction was performed using ReverTra Ace (Toyobo) with antisense primer of $P2X_2$ mRNA, which was designed from +531 of NM_053656, and PCR was carried out with obtained cDNAs and primers for adapter and $P2X_2$ mRNA sequence, which were designed to cross the border of exons 1 and 2. The reaction mixture was electrophoresed in agarose gel, and all of amplicon was gel extracted and restricted by XhoI, whose restriction site was designed in adapter sequence. The fragments were cloned into pcDNA3 vector which restricted by XhoI and EcoRV and sequenced. The adapter and primers sequences are as follows. The 5′-adapter RNA oligonucleotide was 5′-GUCUGAGCUCUCGAGAUAGA-3′; the primer for reverse transcription, 5′-GTTGTCAGAAGTTCCATCCTCCAC-3′; the primer for 5′-adapter, 5′-GTCTGAGCTCTCGAGATAGA-3′; and the reverse primer for target amplification, 5′-CGATGAAGACGTACCACACGAA-3′.

Real-Time Quantitative RT-PCR (TaqMan RT-PCR). Retinoids were dissolved in ethanol and added to the culture medium so that the ethanol represented 0.1% of the v/v concentration. Total cellular RNA was prepared using the RNeasy method from QIAGEN (Valencia, CA) according to the manufacturer's instructions and included an on-column DNase I digestion to minimize genomic DNA contamination. The TaqMan One-Step RT-PCR Master Mix Reagent kit (Applied Biosystems, Foster City, CA) was used with each custom designed, gene-specific primer/probe set to amplify and quantify each transcript of interest. Reactions (25 μl) contained 50 ng of total RNA, 200 nM forward and reverse primers, 100 nM TaqMan probe, and RNase Inhibitor Mix in the Master Mix solution. RT-PCR amplification and real-time detection were performed using an ABI PRISM 7700 sequence detection system (Applied Biosystems) for 30 min at 48°C (reverse transcription), 10 min at 95°C (AmpliTaq Gold activation), 38 cycles of denaturation (15 s at 95°C), and annealing/extension (60 s at 60°C). Data were analyzed using ABI Prism Sequence Detection Software, version 1.1. The following primers and probes were used. The TaqMan probe for $P2X_2R$ was 5′-5-carboxy-

fluorescein-CACTACTCCCAGGATCAGCCACCCA-5-carboxytetramethylrhodamine-3'; the forward primer for $P2X_2R$, 5'-CATATCCCTCCCCCACCTA-3'; and the reverse primer, 5'-GTTGGTCCTTCACCTGATGGA-3'. Sense and antisense primers and probes for GAPDH were obtained from Rodent GAPDH Control Reagents (Applied Biosystems).

Plasmids. The 5'-flanking region of *P2rx2* (described above) was inserted into multicloning sites of the pGL3-basic vector (termed pP2X2luc; Promega). The sequence between two KpnI sites (one site is in the multicloning site and other site is at the −1923 position) in the vector was restricted by KpnI (Takara) and ligated to construct a deletion mutant which lacks 501 bp of the 5' end in the pP2X2luc insert (Del-pP2X2luc). The P2X2-GFP vector was a kind gift from Dr. Murrell-Lagnado (Department of Pharmacology, Cambridge University, Cambridge, UK).

Transient Transfections and Luciferase Assays. Transient transfection was carried out with Superfect (QIAGEN) according to the manufacturer's protocol. Fifty percent confluent cells seeded on 48-well plates were transfected with reporter plasmid (pP2X2luc, Del-pP2X2luc, P2X2-GFP). The phRL-TK vector (Promega) was cotransfected to monitor the transfection efficiency. After 48 h incubation, the cells were lysed. Firefly and *Renilla reniformis* luciferase activity were measured by 1420 ARVOsx multilabel counter (PerkinElmer Wallac, Turku, Finland) using a dual-luciferase reporter assay system (Promega). The transfection efficiency was corrected by normalizing the firefly luciferase activity to the *R. reniformis* luciferase activity.

Western Blot of $P2X_2$ Receptor Protein. After treatment of the cells with 9-*cis*-retinoic acid (9-*cis*-RA) for 1 day, the cells were washed with phosphate-buffered saline(−) twice and lysed in buffer containing 10 mM Tris-HCl, pH 7.4, 150 mM NaCl, 10 mM EDTA, 5 mM EGTA, 0.5% mM Nonidet P-40, and 0.5% deoxycholate. The protein concentration was measured by bicinchoninic acid protein assay (Pierce Chemical, Rockford, IL). Proteins (10–30 μg/lane) were mixed with SDS sample buffer, loaded onto a 10% polyacrylamide gel, electrophoresed, and transferred onto a nitrocellulose membrane. The membrane was then blocked in 5% nonfat dry milk in Tris-buffered saline containing 0.1% Tween 20. The membrane was incubated with the anti-rabbit $P2X_2$ polyclonal antibody (1:200; Calbiochem, San Diego, CA) or β-actin (1:5000; Sigma-Aldrich, St. Louis, MO) overnight at 4°C, followed by incubation with the horseradish peroxidase-conjugated anti-rabbit antibody (1:2000; GE Healthcare, Little Chalfont, Buckinghamshire, UK). The blots were probed with an ECL Western blot detection system (GE Healthcare). Quantification of immunoreactive bands was performed by scanned image analysis on a computer.

Whole Cell Patch-Clamp Recording. The cells were placed in a recording chamber and continuously superfused at room temperature (22–24°C) in an extracellular solution containing 140 mM NaCl, 5.4 mM KCl, 1.8 mM $CaCl_2$, 1.0 mM $MgCl_2$, 11.1 mM D-glucose, and 10 mM HEPES; pH adjusted to 7.4 with NaOH. Patch pipettes were filled with an intracellular solution containing 150 mM CsCl, 10 mM HEPES, and 5 mM EGTA; pH adjusted to 7.3 with CsOH. With this solution, patch electrode resistances ranged between 5 and 8 MΩ. The whole cell patch-clamp was made, and cells were voltage-clamped at −60 mV. ATP was diluted with extracellular solution and applied to the patched cell by gravity from a tube (300-μm inner diameter) attached to an electrically controlled valve. Currents were recorded with an Axopatch 200-B amplifier (Molecular Devices, Sunnyvale, CA) and analyzed using pClamp5 software (Molecular Devices).

Measurement of DA Released from PC-12 Cells. Cells were plated on 35-mm dishes and washed twice with 1 ml of balanced salt solution (BSS) containing 150 mM NaCl, 5 mM KCl, 1.2 mM $CaCl_2$, 1.2 mM $MgCl_2$, 25 mM HEPES, and 10 mM D-glucose and then incubated for 1 h with 1 ml of BSS at room temperature. The cells were again washed with BSS and then stimulated by BSS with or without 30 μM ATP for 1 min. BSS was collected in 1.5-ml tubes loaded with 250 μl of 1 N perchloric acid (PCA), and 1 ml of 0.2 N PCA was added to the dishes and incubated for 2 h on ice. Both the collected PCA solutions were centrifuged, and then the supernatants were used for DA measurement. The amount of DA in the solution was measured using high-performance liquid chromatography combined with electrochemical detection.

Intracellular Calcium Imaging. The increase in $[Ca^{2+}]_i$ in single cells was measured by the fura-2 method with minor modifications. Cells were washed with BSS and incubated with 10 μM fura-2 acetoxymethyl ester at 37°C in BSS for 45 min. The coverslips were mounted on an inverted epifluorescence microscope (TMD-300; Nikon, Tokyo, Japan) equipped with a 75-W xenon lamp and band-pass filters of 340-nm wavelength for measurement of the Ca^{2+}-dependent signal (F_{340}) and 360-nm wavelength for measurement of the Ca^{2+}-independent signal (F_{360}).

Results

Homology Search for Transcription Factor Binding Sites in the 5'-Flanking Region of *P2rx2*. The *P2rx2* is located at rat chromosome 12 and has 11 exons between 5'- and 3'-untranslated region (National Center for Biotechnology Information Entrez GeneID 114115). $P2X_2$ mRNA sequence has been first determined by Brake et al. (1994). Of 11 splicing variants registered in GenBank database, only two variants are reported to express functional channel (*P2rx2*, NM_053656; *P2X 2b*, Y10473). The information of the 5'-flanking region of the rat *P2rx2* was obtained from National Center for Biotechnology Information Rat Genome Resources. In the *Rattus norvegicus* (Norway rat) chromosome 12 genomic contig from whole genome shotgun sequence (NW_047378), putative transcription start site of *P2rx2* is predicted by searching the sequence location of rat $P2X_2$ mRNA (NM_053656) using BLAST. Then, a 2524-bp fragment upstream of the Wistar rat *P2rx2* was cloned in the pGL3 vector. Whether the cloned sequence is located in the 5'-flanking region of *P2rx2* is confirmed by sequencing the 743-bp amplicon obtained by genome PCR using specific primers for the third exon of *P2rx2* and our cloned sequence. The homology between database sequence and the cloned sequence was more than 99.8% match. In the cloned sequence, we found three putative RAREs that conformed with a general canonical sequence in which two directly repeated hexanucleotide motifs [consensus (A/G)G(G/T)TCA] are separated by one (DR1: −2309/−2321), four (DR4: −2299/−2314), and five nucleotides (DR5: −2408/−2424) (Fig. 1). We used TESS to verify these sites and confirmed that they were predicted as RAREs. The sequence analysis using TESS also predicted the presence of many consensus sequences for various transcription factors in the cloned fragment such as simian virus 40 protein 1 (Sp-1), AP-1, AP-2, GATA-1, nuclear factor-κB, and cAMP response element-binding protein binding motifs. Sequence data from the 5'-flanking region of the Wistar rat *P2rx2* have been deposited in GenBank with the accession number AY749416. Furthermore using oligo-capping 5' RACE, we could obtain single sequence that encodes 5' region of $P2X_2$ mRNA, suggesting that transcription starting site of *P2rx2* in PC-12 cells is located in 27 bases upstream of RefSeq sequence (NM_053656). Consensus sequences of GC-box (GGGCGG) and initiator (YYANWYY), which are expected to form core promoter region, were found in −67 and −52 bp upstream of transcription starting site determined with oligo-capping 5' RACE.

$P2X_2$ mRNA Level Is Increased by Retinoids Treatment in PC-12 Cells. The presence of putative RAREs in the 5′-flanking region of the *P2rx2* indicated the possibility that retinoids may change the expression of $P2X_2$ receptors. We examined the level of the $P2X_2$ mRNA expression in PC-12 cells that had been treated with or without 9-*cis*-RA, an active form of an endogenous vitamin A derivative, using real-time quantitative RT-PCR analysis. We found that the $P2X_2$ mRNA in 9-*cis*-RA (100 nM)-treated PC-12 cells was markedly increased and the highest level was observed as early as 3 h later ($n = 4$; ***, $p < 0.001$), and the increase persisted for at least 12 h after the treatment with 9-*cis*-RA ($n = 4$; ***, $p < 0.001$) (Fig. 2A). The increase in the level of $P2X_2$ mRNA by 9-*cis*-RA was dose-dependent, and a significant increase was seen at 100 and 1000 nM 9-*cis*-RA (Fig. 2B).

9-*cis*-RA is known to be an activator of the nuclear receptors RXR and RAR (Aranda and Pascual, 2001). RXR can form as homodimers and as heterodimers with a number of other nuclear receptors such as RAR (Aranda and Pascual, 2001). To clarify the nuclear receptors involved in the increase in the level of $P2X_2$ mRNA, we used two ligands, all-*trans*-retinoic acid (atRA) (Aranda and Pascual, 2001) and PA024 (Takahashi et al., 2002), agonists preferentially of RAR and RXR, respectively. In this experiment, PC-12 cells were cultured in serum-free medium to detect only the effects of RAR and RXR agonists because serum contains large amounts of retinoids and binding protein (Mori, 1978). In this condition, a dose-dependent increase in the level of $P2X_2$ mRNA was also observed in cells treated with 9-*cis*-RA (Fig. 3) as in cells grown in medium with serum (Fig. 2). We treated PC-12 cells with atRA and found that the level of

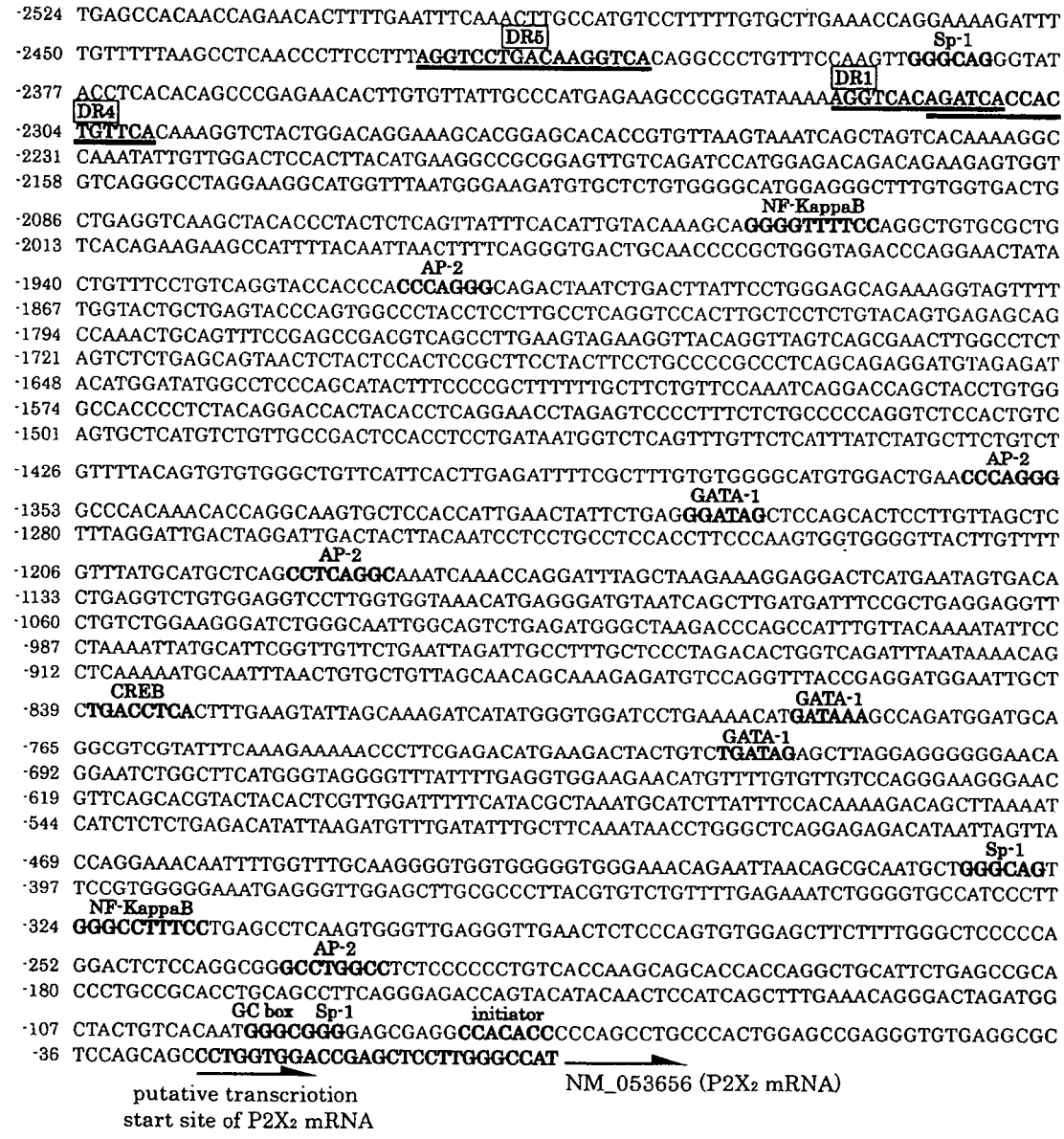

Fig. 1. Nucleotide sequence of the 5′-flanking region of the Wistar rat *P2rx2*. A 2524-base pair genomic sequence of 5′-flanking region of *P2rx2* was cloned and sequenced (GenBank accession no. AY749416) and analyzed to search for consensus motifs interacting with transcription factors using TESS. Predicted RAREs, sequences are underlined and indicated in bold. Other potential transcription binding sites predicted by TESS are indicated in bold. Arrows represent the location of $P2X_2$ mRNA sequences indicated by RefSeq sequence and 5′ RACE analysis.

$P2X_2$ mRNA was markedly increased. The increase was in a dose-dependent manner, and a significant increase was seen at the range of 10 to 1000 nM atRA (Fig. 3). By contrast, the preferential agonist of RXR, PA024 (1–100 nM), did not increase the level of $P2X_2$ mRNA. Because PC-12 cells undergo apoptotic cell death by serum deprivation (Batistatou and Greene, 1993), we maintained cells in serum-containing medium for other experiments.

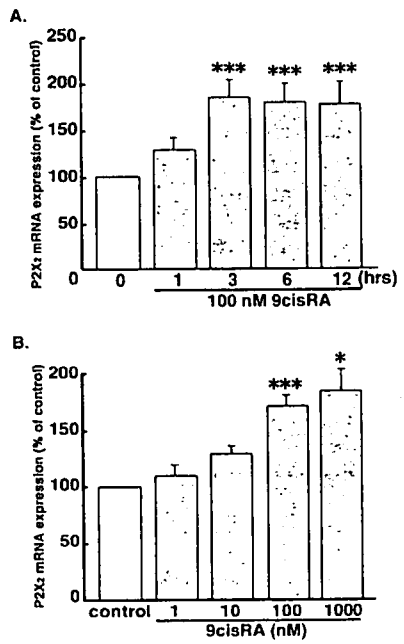

Fig. 2. Increase in the level of $P2X_2$ receptor mRNA by 9-*cis*-retinoic acid. PC-12 cells were treated with 100 nM 9-*cis*-RA for 1, 3, 6, and 12 h (A) or with different concentrations of 9-*cis*-RA (1–1000 nM) (B) followed by real-time RT-PCR analysis of $P2X_2$ and GAPDH mRNAs. $P2X_2$ mRNA levels were normalized by GAPDH mRNA levels, and each set of data represents the means ± S.E.M. of percentages of control from four individual experiments (***, $p < 0.001$; *, $p < 0.05$, multiple comparisons versus control group using Bonferroni t test after one-way ANOVA).

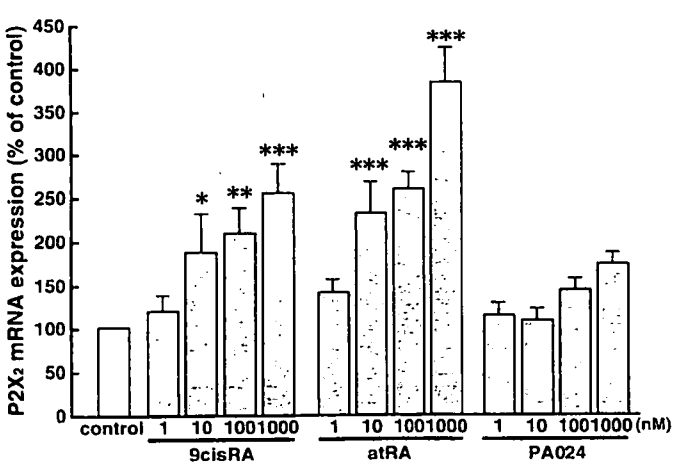

Fig. 3. Effects of selective RAR and RXR agonists on the level of $P2X_2$ receptor mRNA. PC-12 cells were treated with 9-*cis*-RA, atra, or PA024 at different concentrations for 3 h in serum-free condition followed by real-time RT-PCR analysis of $P2X_2$ and GAPDH mRNAs. $P2X_2$ mRNA levels were normalized by the GAPDH mRNA levels, and each set of data represents the means ± S.E.M. of the percentage over the value of the control group from four individual experiments (***, $p < 0.001$; **, $p < 0.01$; *, $p < 0.05$, multiple comparisons versus control group using Bonferroni t test after one-way ANOVA).

Retinoids Stimulate the Promoter Activity Driven by the 5′-Flanking Region of *P2rx2*. To determine whether 9-*cis*-RA increases $P2X_2$ mRNA at the transcriptional level, we examined the transcriptional activity of the 5′-flanking region of *P2rx2* (Fig. 4) using a dual-luciferase reporter assay method. The 5′-flanking region of *P2rx2* (a 2524-bp fragment upstream of the putative transcription start site) was inserted into the multicloning site of the pGL3-basic firefly luciferase assay vector (termed pP2X2luc) (Fig. 4A), which was transiently transfected into PC-12 cells. The cloned sequence increased basal luciferase activity by 25-fold. This confirmed that the sequence can promote downstream transcription. When stimulated with 1 μM 9-*cis*-RA, pP2X2luc exhibited higher luciferase activity (from 25.7 ± 2.1 to 42 ± 2.0, 65% increase; $n = 8$; ***, $p < 0.001$) (Fig. 4B). A similar increase in the luciferase activity was also observed with atRA (from 25.7 ± 2.1 to 34.8 ± 2.9., 35% increase; $n = 8$; ***, $p < 0.001$). These results indicate that 9-*cis*-RA and atRA increase the promoter activity of the cloned 5′-flanking region of *P2rx2*. Furthermore, the increases in luciferase activity by 9-*cis*-RA and atRA were lost in cells transfected with a vector lacking the fragment from −2524 to −1924 (Del-pP2X2luc) where three putative RAREs are located (Fig. 4A). In addition, the pGL3-basic vector without the 5′-flanking region of *P2rx2* showed no transcriptional activity, the RAR agonists caused no change, and basal activity of Del-

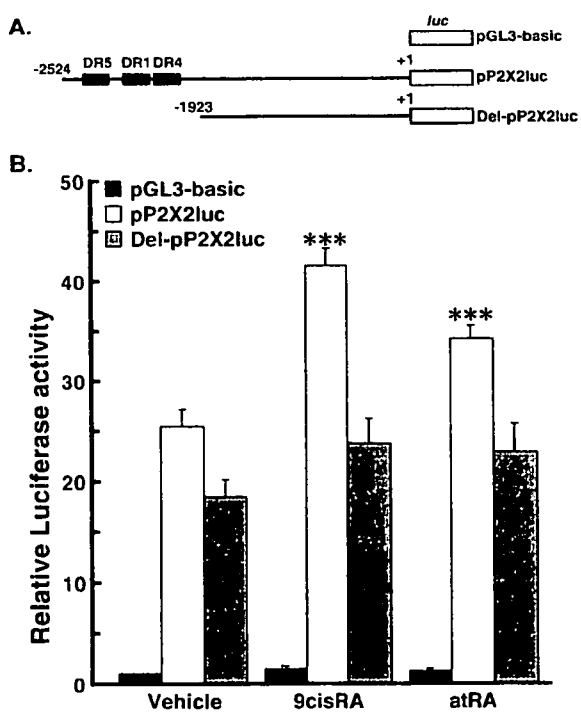

Fig. 4. Transcriptional activity of the 5′-flanking region of *P2rx2* by retinoic acids. The two constructed vectors (pP2X2luc and Del-pP2X2luc) and the empty vector (pGL3-basic) used in the experiment, as described under *Materials and Methods*, are schematically illustrated. Each construct was transfected into PC-12 cells, and the firefly luciferase activity, normalized to the *R. reniformis* luciferase activity driven by the cotransfected phRL-TK, was determined 24 h after the transfection in the presence or absence of 1 μM 9-*cis*-RA or 1 μM atRA (pGL3-basic, open columns; pP2X2luc, closed columns; and Del-pP2X2luc, gray columns). Each value represents the mean ± S.E.M. of the relative light activities to the control treated pGL3-basic vector activity ($n = 8$; ***, $p < 0.001$ by Student-Newman-Keuls method after two-way ANOVA, compared with the value of control group).

pP2X2luc was decreased to 19-fold greater than pGL3, compared with 25-fold grater than pGL3 for pP2X2luc. These results indicate that the RAREs mediate the transcriptional activity of the 5′-flanking region of the *P2rx2* by retinoids.

The Protein Level of $P2X_2$ in PC-12 Cells Is Increased by 9-*cis*-RA Treatment. To investigate whether 9-*cis*-RA increases the level of $P2X_2$ protein as a consequence of an increase in the mRNA level, we performed Western blot analyses to detect $P2X_2$ protein by using a specific antibody for the $P2X_2$ receptor. The specificity of antibody was confirmed by comparing protein blots of 1321N1 cells transfected or untransfected with rP2X2-GFP. In cells transfected with rP2X2-GFP, a single band is detected at approximately 90 kDa, consistent with the molecular mass sum of $P2X_2$ and GFP, whereas no band was detected in untransfected cells. In PC-12 cells, the antibody detected an intense band at approximately 70 kDa with a weak smear ranging from 60 to 80 kDa that was postulated to be glycosylated $P2X_2$ protein. In PC-12 cells that had been treated with 9-*cis*-RA (1–1000 nM) for 24 h, the $P2X_2$ protein was significantly increased in a concentration-dependent manner up to approximately 65% (n = 4–14; *, $p < 0.05$, **, $p < 0.01$) (Fig. 5) in comparison with the level expressed in control. The increase in the $P2X_2$ receptor protein by 9-*cis*-RA was consistent with that in $P2X_2$ mRNA.

9-*cis*-RA Increased the Amplitude of ATP-Evoked Whole-Cell Current in PC-12 Cells. $P2X_2$ receptors form nonselective cation channels, and ATP evokes an inward current (North, 2002). Thus, to investigate whether 9-*cis*-RA increases the level of $P2X_2$ receptors in PC-12 cells as functional channels, we performed whole-cell patch-clamp recordings to examine the ATP-activated inward current. Treatment of cells with 100 nM 9-*cis*-RA for 24 h significantly increased the amplitude of the ATP-evoked inward current (**, $p < 0.01$; Fig. 6, A and B). The concentration-response curves for the ATP-activated currents in control and 9-*cis*-RA-treated cells showed that 9-*cis*-RA did not change the Hill coefficient (control cells, 1.9; 9-*cis*-RA-treated cells, 2.1) and EC_{50} value (control cells, 33; 9-*cis*-RA-treated cells, 30) but enhanced the maximal response (Fig. 6B). Furthermore, 20 μM PPADS almost completely blocked ATP-induced current, which means PPADS-insensitive $P2X_4$ expression is too low to evoke the whole cell current, even though mRNA expression is detectable by RT-PCR. The membrane capacitance, reversal potential, inward rectification property (data not shown), and activation kinetics estimated from the current trace were not significantly changed in the 9-*cis*-RA-treated cells, compared with untreated controls. These results indicate that the expression of functional $P2X_2$ receptors is increased on the plasma membrane of 9-*cis*-RA-treated PC-12 cells.

9-*cis*-RA Facilitates P2X-Mediated $[Ca^{2+}]_i$ Elevation. $P2X_2$ receptors are reported to be highly permeable to Ca^{2+} (Virginio et al., 1998). We monitored the level of $[Ca^{2+}]_i$ in individual PC-12 cells using the Ca^{2+}-sensitive fluorescent

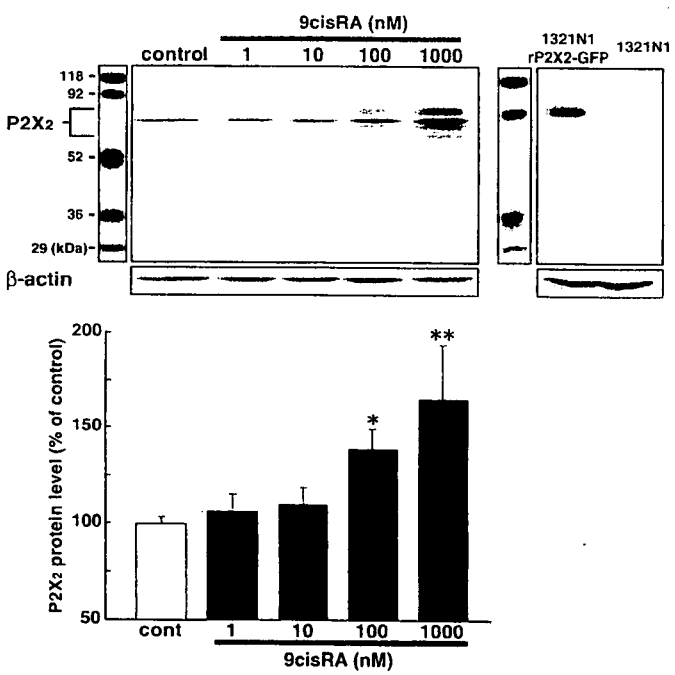

Fig. 5. Increase in $P2X_2$ protein expression by 9-*cis*-RA. Total protein from PC-12 cells treated with or without 9-*cis*-RA (range 1–1000 nM) for 24 h was subjected to Western blot analysis. The proteins of $P2X_2$ receptor and β-actin were detected by their specific antibodies. The intensities of the bands were quantified, and the relative values of $P2X_2$ protein were normalized by the values of the β-actin protein levels for the loading control. The anti-$P2X_2$ antibody was tested on the lysate of 1321N1 cells with or without transfection of P2X2-GFP expression vector. Each set of data represents the mean ± S.E.M. of the percentage over the control (n = 4–14; *, $p < 0.05$; **, $p < 0.01$ by multiple comparisons versus control group using Bonferroni t test after one-way ANOVA).

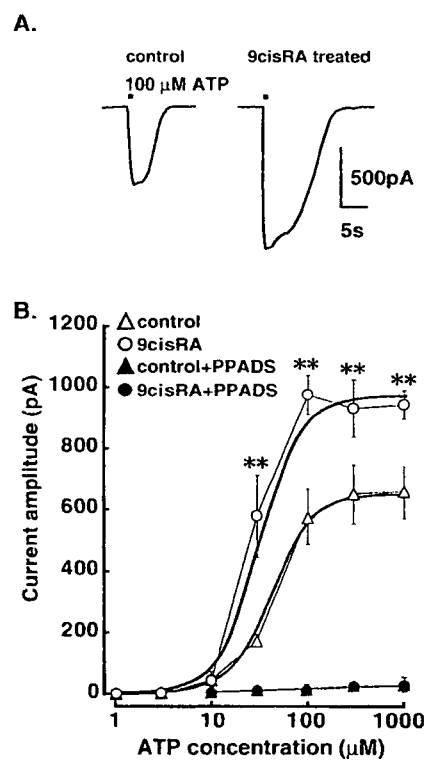

Fig. 6. Effect of 9-*cis*-RA on ATP-induced whole cell current in PC-12 cells. A, representatives traces were the currents evoked by 100 μM ATP in PC-12 cells with or without 100 nM 9-*cis*-RA for 24 h. Cells were voltage-clamped at −60 mV. B, concentration-dependent curves were made by measuring currents elicited by a series of ATP concentrations with or without 20 μM PPADS. Each point represents the mean values ± S.E.M. of the maximum amplitude of the ATP-evoked currents (n = 10–13; **, $p < 0.01$ by t test, compared with the value of the corresponding control group) and was fitted to a sigmoidal curve to calculate Hill coefficient and the EC_{50} values.

dye fura-2 and examined the effects of 9-*cis*-RA on the ATP-evoked $[Ca^{2+}]_i$ elevation. Applying 100 μM ATP produced an increase in the 340/360 emission ratio for fura-2 (n = 21 cells), indicating that ATP caused an increase in $[Ca^{2+}]_i$ in the PC-12 cells (Fig. 7A), as shown previously (Fasolato et al., 1990). Treatment of the cells with 100 nM 9-*cis*-RA for 24 h significantly enhanced the ATP-evoked increase in $[Ca^{2+}]_i$ by approximately 30% (**, $p < 0.01$) (Fig. 7, A and B). PC-12 cells express not only $P2X_2$ but also P2Y (presumably $P2Y_2$) receptors (Raha et al., 1993), both of which increase $[Ca^{2+}]_i$ after their activation. It has been shown that the P2X and P2Y receptor-mediated $[Ca^{2+}]_i$ elevations can be distinguished by using an extracellular recording solution (BSS) without Ca^{2+} to remove P2X component and by treating cells with the phospholipase Cβ inhibitor U-73122 to remove the P2Y component. When Ca^{2+} was not added to the extracellular solution, the increase in $[Ca^{2+}]_i$ evoked by ATP was markedly reduced by ~55% (n = 24 cells) (Fig. 7B). On the other hand, U-73122 (5 μM) reduced the ATP-evoked increase in $[Ca^{2+}]_i$ by approximately 40%. PC-12 cells that had been treated with 9-*cis*-RA did not show any enhancement of the ATP-evoked $[Ca^{2+}]_i$ elevation in the extracellular recording solution without Ca^{2+} but did after treatment with U-73122 (Fig. 7B). Furthermore, inhibition of $P2X_2$ but not $P2X_4$ by 20 μM PPADS reduced ATP-evoked $[Ca^{2+}]_i$ elevation to the level in Ca^{2+}-free BSS both in 9-*cis*-RA-treated or untreated PC-12 cells (Fig. 7B). This result suggests ATP-evoked Ca^{2+} influx through P2X receptors does not include a $P2X_4$ response. Application of 80 mM K^+ evoked the release of DA presumably via activating voltage-dependent Ca^{2+} channels (VDCCs) (Waterman, 2000), but the $[Ca^{2+}]_i$ elevation evoked by 80 mM K^+ was not altered by the treatment with 9-*cis*-RA (Fig. 7B). Together, these results indicate that 9-*cis*-RA up-regulates the expression of $P2X_2$ receptors in PC-12 cells, and activating them by ATP increases Ca^{2+} influx, which contributes to enhancing the neurotransmitter release.

ATP-Induced DA Release from PC-12 Cells Is Enhanced by 9-*cis*-RA Treatment. PC-12 cells are known as a model of neuronal cells (Shafer and Atchison, 1991) and are able to release neurotransmitters such as catecholamines by various extracellular stimuli, including ATP (Nakazawa and Inoue, 1992). The ATP-evoked DA release requires Ca^{2+} influx into cells mediated through opening $P2X_2$ receptor channels but not VDCCs (Inoue et al., 1989). Thus, we investigated whether the ATP-evoked release of DA from PC-12 cells is modulated by 9-*cis*-RA. Stimulation of PC-12 cells with 30 μM ATP for 1 min caused the release of DA as shown previously (Nakazawa and Inoue, 1992). By contrast, in PC-12 cells treated with 100 nM 9-*cis*-RA for 24 h, the ATP-evoked DA release was significantly enhanced by 35.7 ± 7.3% (n = 9; ***, $p < 0.001$; Fig. 8A) without significant change in the total DA content in the cells (94.4 ± 2.4%; p = 0.07; Fig. 8B). 9-*cis*-RA did not affect the spontaneous release of DA from PC-12 cells (control cells, 7.7 ± 2.5%; 9-*cis*-RA-treated cells, 12.8 ± 3.1%; p = 0.23; Fig. 8A).

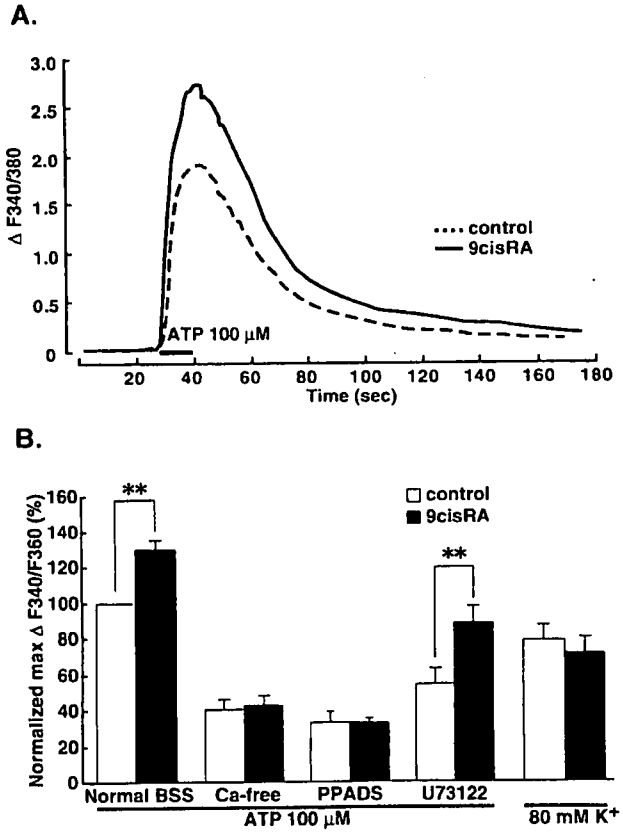

Fig. 7. Effect of 9-*cis*-RA on ATP-induced $[Ca^{2+}]_i$ elevation in PC-12 cells. A, traces showing the records of the fura-2 emission ratios from PC-12 cells onto which 100 μM ATP was applied with or without 100 nM 9-*cis*-RA for 24 h. B, ATP-induced $[Ca^{2+}]_i$ elevations were measured in several different conditions (from left: normal BSS, n = 9; Ca^{2+}-free BSS, n = 5; 20 μM PPADS, n = 3; and 5 μM U-73122, n = 6). To measure the $[Ca^{2+}]_i$ elevation by the depolarizing stimulation, BSS containing a high concentration of potassium (80 mM; n = 5) was applied. Each set of data represents the mean ± S.E.M. of the maximum responses of the ratiometric fura-2 fluorescence ($\Delta F_{340}/\Delta F_{360}$), which were normalized by the value obtained from control PC-12 cells (**, $p < 0.01$ by Student-Newman-Keuls method after two-way ANOVA, compared with the value of control group).

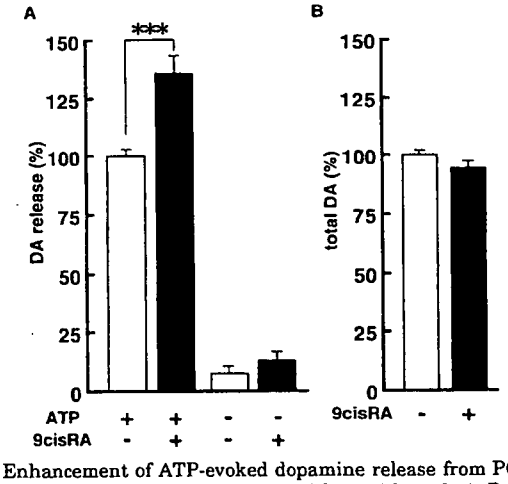

Fig. 8. Enhancement of ATP-evoked dopamine release from PC-12 cells by 9-*cis*-RA. PC-12 cells were incubated with or without 9-*cis*-RA for 24 h. A, the extracellular contents of DA after the application of 30 μM ATP for 1 min were measured with the high-performance liquid chromatography combined with electrochemical detection system. B, measured amount of extracellular and intracellular DA was compared as percentage of 9-*cis*-RA untreated cells. Amount of DA released by ATP was calculated by dividing supernatant values by the sum of supernatant and pellet values and shown as the mean ± S.E.M. of the percentage of the ATP-evoked DA release in 9-*cis*-RA-untreated control cells (n = 9; ***, p < 0.001 by t test).

Discussion

In the present study, we first identified three motifs that are canonical consensus sequences of RAREs in the cloned 5′-flanking region of the Wistar rat *P2rx2* and found that 9-*cis*-RA, an endogenous vitamin A derivative, increases the expression of the $P2X_2$ receptor at the transcriptional level in the neuronal model PC-12 cells. The transcriptional effects of 9-*cis*-RA are primarily mediated by activating two families of nuclear receptors, RARs and RXRs (Chambon, 1996). RXRs can form as homodimers and as heterodimers with a number of other nuclear receptors such as thyroid hormone receptor, vitamin D receptor, and RAR (Aranda and Pascual, 2001). Among them, the RXR/RAR heterodimer is known to respond specifically to the RAR activator atRA (Kurokawa et al., 1994). The present study did not show direct binding of RAR and RXR with 5′-flanking region of *P2rx2* but did demonstrate that atRA-treated PC-12 cells also show an increase in the level of $P2X_2$ mRNA expression, suggesting the involvement of RAR in regulating the $P2X_2$ receptor expression in PC-12 cells. PA024 did not increase the level of $P2X_2$ mRNA. A slight, but not significant, increase in $P2X_2$ mRNA was seen. This finding corresponds with the fact that a low activity of PA024 alone was observed in an experiment of retinoid-induced HL-60 differentiation (Ishida et al., 2003). That PA024 scarcely increased the $P2X_2$ mRNA expression is consistent with the findings of previous studies showing that a single application of RXR-selective agonists does not induce gene transcription (Minucci et al., 1997; Ishida et al., 2003) and is supported by the notion that the RXR ligand induces homodimerization of RXR and inhibits heterodimerization without dimerization partner ligands; moreover, a partner ligand is sufficient for heterodimerization (Dong and Noy, 1998). The RXR/RAR heterodimer generally binds to the DR5 RARE (Kurokawa et al., 1994) and also binds to DR1 (Kurokawa et al., 1994). We determined the $P2X_2$ mRNA transcription start site by 5′ RACE, which is located near the site supposed by RefSeq entry (NM_053656). We also had the predictions for some transcription factor binding sites in the 5′-flanking region of the rat *P2rx2* cloned in the current study, which include the DR5 and DR1 sequences located at −2381/−2397 and −2292/−2294 from the transcription start site. It includes other factors such as simian virus 40 protein 1, activator protein-2, nuclear factor-κB, GATA-1, cAMP response element binding protein, GC-box, and initiator sequence as well. Consensus sequences for GC-box and initiator found in our cloned sequence imply that core promoter region would exist near the 5′ end of our cloned sequence. Although the factors we showed here were just the candidates estimated by the electrical search system, we confirmed that the cloned fragment has sensitivity to retinoid treatment and deletion of a fragment containing DR elements lead to abolishing the 9-*cis*-RA- and atRA-mediated and parts of basal transcriptional activities. On the other hand, the deleted fragment also contains DR4, but this is known as a binding site of RXR heterodimerized with nuclear receptors other than RARs (Aranda and Pascual, 2001). Because RAR/RAR homodimerization has not been reported, our series of results could suggest that retinoic acids activate RAR/RXR heterodimers that bind to RAREs (DR5 and/or to DR1-responsive elements) located at the distant place from transcription start site in the promoter region of the *P2rx2*, which in turn work as activators of basal transcription machinery and lead to an increase in the transcription of $P2X_2$ receptors in PC-12 cells.

The biochemical analysis in the present study indicated that the increase in $P2X_2$ transcription resulted in an increase in the level of $P2X_2$ protein. Furthermore, we found that the maximal responses of ATP-evoked currents were enhanced in 9-*cis*-RA-treated PC-12 cells. The inward currents evoked by ATP in PC-12 cells have been demonstrated to be inhibited by suramin, PPADS, and reactive blue 2 (Inoue et al., 1991a,b), a pharmacological profile that fits rat $P2X_2$ receptors, thus suggesting an increase in the level of functional $P2X_2$ protein. This view is strongly supported by the finding that the Ca^{2+} response evoked by ATP in 9-*cis*-RA-treated PC-12 cells was enhanced in the presence of a phospholipase Cβ inhibitor, which abolishes P2Y-mediated Ca^{2+} responses. It could be possible that ATP produces an inward current via activating another P2X subtype. Indeed, in addition to $P2X_2$ receptors $P2X_4$ transcript was also detected in PC-12 cells by our RT-PCR analysis (our unpublished observation). However, 20 μM PPADS almost completely blocked ATP-induced inward currents and $[Ca^{2+}]_i$ elevation, and 9-*cis*-RA did not alter the EC_{50} and Hill coefficient value of the ATP-evoked currents in the PC-12 cells. It is suggested that functional $P2X_4$ receptor is not expressed on the cell membrane. In addition, the mRNA level of the $P2X_4$ receptor in the PC-12 cells was not changed by treatment with 9-*cis*-RA (our unpublished observation). In human cervical epithelial cells, however, the expression of $P2X_4$ mRNA has been reported to be increased by atRA (Gorodeski, 2002). This discrepancy may be due to differences in the species, the basal expression levels of $P2X_4$ receptors, and the expression of RAR and RXR isoforms or the large numbers of coregulators.

In the nervous system, a key function of $P2X_2$ receptors is to increase release of neurotransmitters (Khakh et al., 2003). PC-12 cells are frequently used in studies investigating stimulus-induced vesicular transmitter release (Shafer and Atchison, 1991). We have observed that retinoid significantly enhanced the ATP-evoked release of DA from PC-12 cells. Because retinoid treatment might lead to the changes in many gene transcriptions involved in $[Ca^{2+}]_i$ elevation, exocytotic machinery, or packaging in vesicles, the enhancement of DA release seen in the present study might include multiple interpretations. However, we found that enhancement by 9-*cis*-RA of the $P2X_2$ receptor protein expression level and ATP-activated Ca^{2+} entry was almost identical to that of the ATP-evoked DA release. In addition, 9-*cis*-RA did not affect basal release or the total content of DA in PC-12 cells, suggesting the 9-*cis*-RA affects neither DA biosynthesis nor exocytotic machinery itself. Calcium is one of the most important factors to regulate exocytosis, and we previously showed that the ATP-evoked DA release from PC-12 cells is induced by Ca^{2+} influx directly via $P2X_2$ channels but not via VDCCs (Nakazawa and Inoue, 1992). Together with this, the most probable interpretation of the results could be that 9-*cis*-RA up-regulates $P2X_2$ receptor mRNAs and proteins, thereby leading to enhancement of $P2X_2$ receptor-mediated Ca^{2+} entry and DA release in PC-12 cells.

In native neurons, activating P2X receptors on the presynapses facilitates the release of neurotransmitters by directing Ca^{2+} influx through P2X receptors (Shigetomi and Kato,

2004). This raises the possibility that retinoids may increase the synaptic effects of ATP in modulating neurotransmitter release in native neurons by up-regulating $P2X_2$ receptors. In the adult brain, relatively high levels of retinoic acid are detected (Werner and Deluca, 2002). In particular, in the hippocampal region it has been shown that molecules required for retinoid signaling pathways are expressed (MacDonald et al., 1990; Werner and Deluca, 2002). These include cellular retinol binding proteins that facilitate retinol uptake into cells; retinal dehydrogenases, which are enzymes for the synthesis of retinoids; and cellular retinoic acid binding proteins, which are thought to deliver atRA to RAR in cell nuclei, as well as RARs and RXRs (Dong et al., 1999). The hippocampus is one of the areas where the roles of $P2X_2$ receptors in facilitating neurotransmitter release have been investigated (Khakh et al., 2003; Shigetomi and Kato, 2004). One can question that retinoid effect on the PC-12 cells is the consequence of the differentiation of PC-12 into neurons. However, morphological differentiation of PC-12 cells by retinoic acid requires a period of greater than 3 weeks, and retinoic acid treatment increased differentiation of nerve growth factor-stimulated PC-12 cells (Boniece and Wagner, 1995). Thus, retinoic acid-induced differentiation of PC-12 cells was suggested to be the consequence of complicated molecular modulations. In fact, we observed up-regulation of $P2X_2$ mRNA within 3 h after retinoids treatment. Hence, the effect of retinoids on $P2X_2$ expression could be a notable factor for the differentiation, but it might be distinguished from differentiation of PC-12 cells. The up-regulation of $P2X_2$ receptors by retinoids may be involved in some of the biological effects of retinoids in neuronal function and synaptic plasticity in the nervous system (Wang et al., 2004).

In the present study, we found that the $P2X_2$ receptor is up-regulated by retinoids as a result of increased transcription most likely mediated by the retinoid-activated RAR heterodimerized with RXR acting on RAREs (presumably DR5- and DR1-responsive elements) in the promoter region of *P2rx2* in neuronal cells. An increase in the expression of $P2X_2$ receptors in neuronal cells has recently been implicated in the development of several pathological states, such as brain ischemia (Cavaliere et al., 2003) and chronic pain (Xu and Huang, 2002), and $P2X_2$ receptor might thus be a target for their treatment. It is noteworthy that in an analysis of the human genomic sequence using TESS, we also found a putative DR5-responsive element in the 5′-flanking region of the human *P2X₂* gene. Together, the present results provide the molecular mechanism underlying the expression of $P2X_2$ receptors and may help in understanding the roles of $P2X_2$ receptors in the regulation of neuronal function, synaptic plasticity, and pathophysiology in the nervous system.

Acknowledgments

We thank Dr. Satoko Ohkubo for helpful discussion, Tomoko Obama for assistance with the cell cultures, Yukari Sigemoto-Mogami for technical suggestions, and Dr. Murrell-Lagnado for providing the P2X2-GFP vector.

References

Aranda A and Pascual A (2001) Nuclear hormone receptors and gene expression. *Physiol Rev* 81:1269–1304.

Batistatou A and Greene LA (1993) Internucleosomal DNA cleavage and neuronal cell survival/death. *J Cell Biol* 122:523–532.

Boniece IR and Wagner JA (1995) NGF protects PC12 cells against ischemia by a mechanism that requires the N-kinase. *J Neurosci Res* 40:1–9.

Boue-Grabot E, Barajas-Lopez C, Chakfe Y, Blais D, Belanger D, Emerit MB, and Seguela P (2003) Intracellular cross talk and physical interaction between two classes of neurotransmitter-gated channels. *J Neurosci* 23:1246–1253.

Brake AJ, Wagenbach MJ, and Julius D (1994) New structural motif for ligand-gated ion channels defined by an ionotropic ATP receptor. *Nature (Lond)* 371:519–523.

Cavaliere F, Florenzano F, Amadio S, Fusco FR, Viscomi MT, D'Ambrosi N, Vacca F, Sancesario G, Bernardi G, Molinari M, et al. (2003) Up-regulation of $P2X_2$, $P2X_4$ receptor and ischemic cell death: prevention by P2 antagonists. *Neuroscience* 120:85–98.

Chambon P (1996) A decade of molecular biology of retinoic acid receptors. *FASEB J* 10:940–954.

Dong D and Noy N (1998) Heterodimer formation by retinoid X receptor: regulation by ligands and by the receptor's self-association properties. *Biochemistry* 37: 10691–10700.

Dong D, Ruuska SE, Levinthal DJ, and Noy N (1999) Distinct roles for cellular retinoic acid-binding proteins I and II in regulating signaling by retinoic acid. *J Biol Chem* 274:23695–23698.

Fasolato C, Pizzo P, and Pozzan T (1990) Receptor-mediated calcium influx in PC12 cells. ATP and bradykinin activate two independent pathways. *J Biol Chem* 265:20351–20355.

Fujiwara Y and Kubo Y (2004) Density-dependent changes of the pore properties of the $P2X_2$ receptor channel. *J Physiol (Lond)* 558:31–43.

Galligan JJ and Bertrand PP (1994) ATP mediates fast synaptic potentials in enteric neurons. *J Neurosci* 14:7563–7571.

Gorodeski GI (2002) Expression, regulation and function of $P2X_4$ purinergic receptor in human cervical epithelial cells. *Am J Physiol* 282:C84–C93.

Illes P and Alexandre Ribeiro J (2004) Molecular physiology of P2 receptors in the central nervous system. *Eur J Pharmacol* 483:5–17.

Inoue K and Kenimer JG (1988) Muscarinic stimulation of calcium influx and norepinephrine release in PC12 cells. *J Biol Chem* 263:8157–8161.

Inoue K, Nakazawa K, Fujimori K, and Takanaka A (1989) Extracellular adenosine 5′-triphosphate-evoked norepinephrine secretion not relating to voltage-gated Ca channels in pheochromocytoma PC12 cells. *Neurosci Lett* 106:294–299.

Inoue K, Nakazawa K, Ohara-Imaizumi M, Obama T, Fujimori K, and Takanaka A (1991a) Antagonism by reactive blue 2 but not by brilliant blue G of extracellular ATP-evoked responses in PC12 phaeochromocytoma cells. *Br J Pharmacol* 102: 851–854.

Inoue K, Nakazawa K, Ohara-Imaizumi M, Obama T, Fujimori K, and Takanaka A (1991b) Selective and competitive antagonism by suramin of ATP-stimulated catecholamine-secretion from PC12 phaeochromocytoma cells. *Br J Pharmacol* 102:581–584.

Ishida S, Shigemoto-Mogami Y, Kagechika H, Shudo K, Ozawa S, Sawada J, Ohno Y, and Inoue K (2003) Clinically potential subclasses of retinoid synergists revealed by gene expression profiling. *Mol Cancer Ther* 2:49–58.

Kanjhan R, Housley GD, Burton LD, Christie DL, Kippenberger A, Thorne PR, Luo L, and Ryan AF (1999) Distribution of the $P2X_2$ receptor subunit of the ATP-gated ion channels in the rat central nervous system. *J Comp Neurol* 407:11–32.

Khakh BS, Gittermann D, Cockayne DA, and Jones A (2003) ATP modulation of excitatory synapses onto interneurons. *J Neurosci* 23:7426–7437.

Khakh BS, Zhou X, Sydes J, Galligan JJ, and Lester HA (2000) State-dependent cross-inhibition between transmitter-gated cation channels. *Nature (Lond)* 406: 405–410.

Kurokawa R, DiRenzo J, Boehm M, Sugarman J, Gloss B, Rosenfeld MG, Heyman RA, and Glass CK (1994) Regulation of retinoid signalling by receptor polarity and allosteric control of ligand binding. *Nature (Lond)* 371:528–531.

MacDonald PN, Bok D, and Ong DE (1990) Localization of cellular retinol-binding protein and retinol-binding protein in cells comprising the blood-brain barrier of rat and human. *Proc Natl Acad Sci USA* 87:4265–4269.

Maruyama K and Sugano S (1994) Oligo-capping: a simple method to replace the cap structure of eukaryotic mRNAs with oligoribonucleotides. *Gene* 138:171–174.

Minucci S, Leid M, Toyama R, Saint-Jeannet JP, Peterson VJ, Horn V, Ishmael JE, Bhattacharyya N, Dey A, Dawid IB, et al. (1997) Retinoid X receptor (RXR) within the RXR-retinoic acid receptor heterodimer binds its ligand and enhances retinoid-dependent gene expression. *Mol Cell Biol* 17:644–655.

Mori T (1978) Study of a growth factor for *Mycobacterium lepraemurium*. I. Minimal medium. *Int J Lepr Other Mycobact Dis* 46:125–132.

Nakazawa K and Inoue K (1992) Roles of Ca^{2+} influx through ATP-activated channels in catecholamine release from pheochromocytoma PC12 cells. *J Neurophysiol* 68:2026–2032.

North RA (2002) Molecular physiology of P2X receptors. *Physiol Rev* 82:1013–1067.

Raha S, de Souza LR, and Reed JK (1993) Intracellular signalling by nucleotide receptors in PC12 pheochromocytoma cells. *J Cell Physiol* 154:623–630.

Rodrigues RJ, Almeida T, Richardson PJ, Oliveira CR, and Cunha RA (2005) Dual presynaptic control by ATP of glutamate release via facilitatory $P2X_1$, $P2X_{2/3}$, and $P2X_3$ and inhibitory $P2Y_1$, $P2Y_2$ and/or $P2Y_4$ receptors in the rat hippocampus. *J Neurosci* 25:6286–6295.

Rubio ME and Soto F (2001) Distinct Localization of P2X receptors at excitatory postsynaptic specializations. *J Neurosci* 21:641–653.

Shafer TJ and Atchison WD (1991) Transmitter, ion channel and receptor properties of pheochromocytoma (PC12) cells: a model for neurotoxicological studies. *Neurotoxicology* 12:473–492.

Shigetomi E and Kato F (2004) Action potential-independent release of glutamate by Ca^{2+} entry through presynaptic P2X receptors elicits postsynaptic firing in the brainstem autonomic network. *J Neurosci* 24:3125–3135.

Takahashi B, Ohta K, Kawachi E, Fukasawa H, Hashimoto Y, and Kagechika H (2002) Novel retinoid X receptor antagonists: specific inhibition of retinoid synergism in RXR-RAR heterodimer actions. *J Med Chem* 45:3327–3330.

Virginio C, North RA, and Surprenant A (1998) Calcium permeability and block at homomeric and heteromeric $P2X_2$ and $P2X_3$ receptors and P2X receptors in rat nodose neurones. *J Physiol (Lond)* 510:27–35.
Wang Y, Haughey NJ, Mattson MP, and Furukawa K (2004) Dual effects of ATP on rat hippocampal synaptic plasticity. *Neuroreport* 15:633–636.
Waterman SA (2000) Voltage-gated calcium channels in autonomic neuroeffector transmission. *Prog Neurobiol* 60:181–210.
Werner EA and Deluca HF (2002) Retinoic acid is detected at relatively high levels in the CNS of adult rats. *Am J Physiol* 282:E672–E678.
Xu GY and Huang LY (2002) Peripheral inflammation sensitizes P2X receptor-mediated responses in rat dorsal root ganglion neurons. *J Neurosci* 22:93–102.

Address correspondence to: Dr. Kazuhide Inoue, Department of Molecular and System Pharmacology, Graduate School of Pharmaceutical Sciences, Kyushu University, 3-1-1 Maidashi, Higashi, Fukuoka 812-8582, Japan. E-mail: inoue@phar.kyushu-u.ac.jp

Available online at www.sciencedirect.com
SCIENCE DIRECT
Journal of Controlled Release 113 (2006) 271–278
journal of controlled release
www.elsevier.com/locate/jconrel

The short consensus repeats 1 and 2, not the cytoplasmic domain, of human CD46 are crucial for infection of subgroup B adenovirus serotype 35

Fuminori Sakurai [a], Sayaka Murakami [a,b], Kenji Kawabata [a], Naoki Okada [c], Akira Yamamoto [b], Tsukasa Seya [d], Takao Hayakawa [e], Hiroyuki Mizuguchi [a,c,*]

[a] *Laboratory of Gene Transfer and Regulation, National Institute of Biomedical Innovation, Osaka, 567-0085, Japan*
[b] *Department of Biopharmaceutics, Kyoto Pharmaceutical University, Kyoto, 607-8414, Japan*
[c] *Graduate School of Pharmaceutical Sciences, Osaka University, Osaka, 565-0871, Japan*
[d] *Department of Microbiology and Immunology, Graduate School of Medicine, Hokkaido University, Sapporo, 060-8638, Japan*
[e] *Pharmaceuticals and Medical Devices Agency, Tokyo, 100-0013, Japan*

Received 21 October 2005; accepted 8 May 2006
Available online 21 June 2006

Abstract

Human CD46 (membrane cofactor protein) has recently been identified to be an attachment receptor for subgroup B adenoviruses (Ads); however, the precise interaction between human CD46 and subgroup B Ads are just beginning to be understood. In this study, to characterize the interaction between human CD46 and subgroup B Ads, varieties of mutant CD46 were tested for their ability to act as a receptor for Ad serotype 35 (Ad35), which belongs to subgroup B. In addition, we determined Ad35 vector-mediated transgene expression and cellular uptake of Ad35 vectors in the presence of a set of anti-CD46 antibodies. Our data demonstrated that the short consensus repeats (SCRs) 1 and 2 in human CD46 are important for interaction with Ad35, whereas the cytoplasmic domain of human CD46 was found not to be required for the function as an Ad35 receptor. Rather, a complete deletion of the cytoplasmic domain of human CD46 increased the transduction efficiencies of Ad35 vectors. This information should help in elucidation of the mechanism of subgroup B Ad infection, as well in the improvement of the subgroup B Ad vectors.

Keywords: Adenovirus serotype 35 vector; CD46; Short consensus repeat; Cytoplasmic tail; Gene therapy

1. Introduction

Human adenoviruses (Ads) compose a large family of non-enveloped, double-stranded DNA viruses that are a significant cause of acute respiratory, gastrointestinal, and ocular infections in humans. So far, at least 51 serotype Ads have been identified and classified into six distinct subgroups (A–F) [1,2]. Among them, subgroup B is further subdivided into subspecies B1 and B2 on the basis of various biophysical and biochemical criteria. Among the 51 human Ad serotypes, the Ad vector most commonly used for gene transfer is composed of Ad serotype 5 (Ad5), which belongs to subgroup C. Ad5 vectors are very powerful and useful vehicles, but recent studies have revealed that they also have some disadvantages, such as high seroprevalence toward Ad5 in adult populations and low infection activity in cells lacking a primary receptor for Ad5, coxsackievirus and adenovirus receptor (CAR). On the other hand, subgroup B Ads have unique properties that are distinct from those of other subgroup Ads, and that are highly attractive features as a framework for alternative gene delivery vehicles. First, subgroup B Ads have been identified as having lower prevalence than the Ads of other subgroups. The seroprevalences toward most subgroup B Ads is less than 20% in healthy blood donors, while more than 70% of serum samples from healthy donors are positive for anti-Ad5 antibody [3]. This indicates that transduction with Ad vectors based on subgroup B is unlikely to be inhibited by preexisting anti-Ad antibodies. Second, subgroup B Ads utilize human CD46 (membrane cofactor protein) as a cellular receptor for infection [4,5], while other subgroup Ads recognize CAR. Human CD46 is ubiquitously expressed in human cells, suggesting that subgroup

* Corresponding author. Laboratory of Gene Transfer and Regulation, National Institute of Biomedical Innovation, 7-6-8 Asagi, Saito, Ibaragi-City, Osaka, 567-0085, Japan. Tel.: +81 72 641 9815; fax: +81 72 641 9816.
E-mail address: mizuguch@nibio.go.jp (H. Mizuguchi).

0168-3659/$ - see front matter © 2006 Elsevier B.V. All rights reserved.
doi:10.1016/j.jconrel.2006.05.007

B Ad vectors would have a broad tropism for human cells. We have previously developed an Ad vector composed of Ad serotype 35 (Ad35), which belongs to subgroup B [6,7], and have demonstrated that Ad35 vectors exhibit a wider tropism for human cells, including CAR-negative cells, than Ad5 vectors [7].

Human CD46 is a type I transmembrane glycoprotein expressed in almost all human cells, except for erythrocytes. Human CD46 is composed of four cysteine-rich short consensus repeats (SCRs), a serine–threonine–proline-rich (STP) region, a short region of unknown function, a hydrophobic transmembrane domain, and a carboxy-terminal cytoplasmic domain. Alternative splicing in the STP region and the cytoplasmic domain gives rise to four major isoforms of human CD46 (BC1, BC2, C1, and C2). All the isoforms function as cofactors for the plasma serine protease factor I by binding to the complement factors C3b and C4b deposited on self tissue [8,9]. By promoting the proteolytic degradation of these factors, these isoforms protect the cells from complement attack [10,11]. In addition to this function, human CD46 has been identified to be a receptor for several human pathogens: measles virus (MV), human herpesvirus 6 (HHV6), human subgroup B Ads, and two types of bacteria [4,5,12–15]. Among these pathogens, the interactions between human CD46 and MV, HHV6, and pathogenic *Neisseria* have been well studied. MV-binding residues are located on SCR1 and SCR2 [16,17], while SCR3 and 4 are essential for binding of HHV6 to human CD46 [18]. The cytoplasmic domain of CD46 is not required for infection of both MV and HHV6 [18,19]. However, it still remains unknown which domains in human CD46 play an important role in the interaction with subgroup B Ads. Elucidation of the interaction between subgroup B Ads and CD46 would lead to improvement of the Ad vectors that are composed of subgroup B Ads.

In this study, the transduction experiments with Ad35 vectors expressing luciferase were performed using cells expressing a variety of human CD46 mutants in order to map the domains which interact with Ad35. Furthermore, cells expressing wild-type CD46 were transduced with Ad35 vectors in the presence of monoclonal anti-human CD46 antibodies which recognize different SCRs of human CD46. Finally, involvement of the cytoplasmic domain of human CD46 with infection of Ad35 was evaluated.

2. Materials and methods

2.1. Cells and antibodies

Chinese hamster ovary (CHO) cells and CHO transformants stably expressing wild-type CD46, CD46 SCR deletion mutants [16], or cytoplasmic tail deletion mutants were grown in Ham's F-12 medium with 10% fetal bovine serum. Cytoplasmic tail deletion mutants (ΔCyt0 and ΔCyt6 mutants) were stable CHO transformants generated by the transfection of pcDNA-CD46ΔCyt0 and pcDNA-CD46ΔCyt6 (described below) into CHO cells and selection with hygromycin (GIBCO-BRE, Rockville, MD). Monoclonal antibodies against human CD46 SCR1, E4.3, MEM-258, and J4-48 were purchased from Pharmingen (San Diego, CA), Serotec Ltd. (Oxford, United Kingdom), and Immunotech (Marseille, France), respectively. SCR2-specific antibody M177 and SCR3-specific antibody M160 were described previously [20]. The monoclonal anti-CD46 antibodies used in this study and their recognition sites are listed on Table 1.

2.2. Plasmids

The plasmid pcDNA-CD46C2, which contains the human CD46 C2 isoform gene, was constructed as follows. The cDNA of the human CD46 C2 isoform was amplified by PCR using the following primers: CD46-forward, 5′-ATG GAG CCT CCC GGC CGC CGC GAG TGT CCC-3′; CD46-reverse, 5′-CGC GGC CGC CTA TTC AGC CTC TCT GCT CTG CTG-3′. The PCR product was cloned into the *Pme*I site of pcDNA3.1-Hyg(+) (Invitrogen, Carlsbad, CA). The cDNA of the CD46 mutant lacking the cytoplasmic tail (amino acid residues 347–369) (CD46ΔCyt0) was prepared by PCR using the parent CD46 C2 cDNA as a template. The following primers were used for PCR: CD46-forward (described above); and CD46TM-reverse, 5′-GCG GCC GCT CAG TAC GGG ACA ACA CAA ATT ACT GCA AC-3′. The PCR product was cloned into the *Pme*I site of pcDNA3.1-Hyg(+), resulting in pcDNA-CD46ΔCyt0. The plasmid pcDNA-CD46ΔCyt6, which contains a human CD46 C2 isoform lacking a portion of the cytoplasmic domain (amino acid residues 352–369) (CD46ΔCyt6), was constructed in a similar manner using the following primers: CD46-forward (described above); and CD46TM6-reverse, 5′-GCG GCC GCT CAC CTC CTT TGA AGA TAT CTG TAC GGG AC-3′. The sequences of all the constructs were confirmed by DNA sequencing.

2.3. Flowcytometric analysis of CD46 expression

Several CHO cell transformants suspended in staining buffer (phosphate buffered saline (PBS) buffer containing 1% bovine serum albumin (BSA)) were incubated with mouse anti-human CD46 antibodies (E4.3, M177, and M160) for 1 h. Subsequently, the cells were reacted with phycoerythrin (PE)-labeled secondary anti-mouse IgG antibody (Pharmingen). After washing with the staining buffer, the stained cells (10^4 cells) were analyzed using a FACSCalibur and CellQuest software (Becton Dickinson, Tokyo, Japan). For evaluation of Ad35 vector-mediated downregulation of CD46, the CHO transformants were transduced with Ad35L at 3000 vector particles (VP)/cell for 1.5 h as described below. After a 1.5-h incubation, CD46 expression levels in the cells were measured using flowcytometry as described above.

Table 1
Monoclonal anti-CD46 antibodies used in this study

Anti-CD46 antibodies	Recognition domain
E4.3	SCR1
J4-48	SCR1
MEM-258	SCR1
M177	SCR2
M160	SCR3

2.4. Adenovirus vectors

Ad35 vectors expressing luciferase, Ad35L, were prepared by an improved ligation method as previously described [21]. Briefly, the luciferase-expressing Ad35 vector plasmid pAdMS4-CMVL2 was constructed by ligating I-*Ceu*I/PI-*Sce*I-digested pAdMS4 with I-*Ceu*I/PI-*Sce*I-digested pCMVL1 [22]. pAdMS4-CMVL2 was digested with *Sbf*I and the linearized DNA was transfected into VK10-9 cells (kindly provided by Dr. V. Krougliak) [23]. Ad35L were generated 10–14 days after transfection, amplified and purified as described previously [6,7]. Determination of virus particle titers was accomplished spectrophotometrically by the method of Maizel et al. [24].

2.5. Transduction experiments

CHO cells and CHO transformants stably expressing wild-type CD46 or CD46 mutants lacking SCRs or the cytoplasmic tail were seeded at 1×10^4 cells/well into a 96-well plate. On the following day, the cells were transduced with Ad35L at 3000 VP/cell for 1.5 h. Forty-eight hours later, luciferase productions in the cells were measured using a luciferase assay system (PicaGene LT2.0, Toyo Inki Co. Ltd., Tokyo, Japan).

For antibody blocking experiments, CHO transformant expressing CD46 C2 isoform, which was seeded at 1×10^4 cells/well in a 96-well plate the day before transduction, was preincubated with the medium containing anti-CD46 antibodies (E4.3, MEM-258, J4-48, M177, and M160) at the indicated concentrations at 4 °C for 1 h. Ad35L was then added at 3000 VP/cell and left for 1.5 h at 4 °C, after which the cells were washed and incubated at 37 °C. Luciferase productions in the cells were measured 48 h after transduction as described above.

2.6. Real-time quantitative PCR

CHO cells and CHO transformants were seeded at 1×10^5 cells/well into a 12-well plate. On the following day, the cells were transduced with Ad35L as described above. After a 48-h incubation, the cells were washed with PBS, harvested, and pelleted. Total DNA, including the Ad35 vector DNA, was extracted from the cells using a Tissue DNeasy Kit (Qiagen, Valencia, CA, USA). The quantitative real-time PCR was performed with 25 ng of sample DNA, 0.5 μM each primer, 0.16 μM TaqMan probe, and 25 μl of TaqMan universal PCR master mix (Applied Biosystems, Foster City, CA, USA) in a final volume of 50 μl using the ABI Prism 7000 sequence detection system (Applied Biosystems). The PCR was initially denatured at 95 °C for 10 min and then subjected to cycles of 95 °C for 15 s and 60 °C for 1 min. The reaction was carried out for 50 cycles. Primers for amplification were located in the pIX region of Ad35 genome. The sequences of the primers and probe used were as follows: forward, 5′-TGGATGGAAGACCC GTTCAA-3′; reverse, 5′-CGTCCAAAGGTGAAGAACTTA AAGT-3′; probe, 5′ FAM-CGCCAATTCTTCAACGCTGACC TATGC-TAMRA 3′. These sequences were designed using Primer Express software version 1.0 (Applied Biosystems), and it was confirmed that they amplified the products of desired size. The Ad35 vector plasmid pAdMS4 was used as a standard.

3. Results

3.1. Ad35 vector-mediated transduction on CHO transformants expressing CD46 deletion mutants

First, we examined which SCR domains of human CD46 (Fig. 1) are essential for infection of Ad35 using CHO transformants expressing CD46 deletion mutants [16]. Before the transduction experiments, CD46 expression levels and SCR deletion on CHO transformants were confirmed by flowcytometric analysis using anti-CD46 antibodies against each of the SCRs. We found the sufficient levels of CD46 mutant expression for all the clones (Fig. 2). The combined use of several anti-CD46 antibodies demonstrated that the corresponding SCR domains were properly deleted on the CHO transformants. Deletion of SCR4 on the ΔSCR4 mutant was confirmed by RT-PCR and DNA sequence, because the SCR4-specific antibody was not obtained (data not shown).

Next, transduction experiments with Ad35 vectors on CHO transformants were performed. Transduction with Ad35L in ΔSCR1 and ΔSCR2 mutants resulted in approximately 50% of the luciferase production obtained in CHO-CD46 cells, which express full-length CD46. The decreases in the transduction efficiencies in ΔSCR1 and ΔSCR2 mutants were similar. In contrast, the ΔSCR3 and ΔSCR4 mutants produced amounts of luciferase similar to those in CHO-CD46 cells after Ad35L transduction (Fig. 3). Real-time PCR analysis also demonstrated that the uptake of Ad35L was significantly reduced by 58% and by 45% in ΔSCR1 and ΔSCR2 mutants, respectively, compared with CHO-CD46 cells, in contrast, ΔSCR3 and ΔSCR4 mutants exhibited the levels of Ad35 vector uptake similar to CHO-CD46 cells (Fig. 4). These results suggested that SCR1 and 2 are involved with Ad35 infection.

3.2. Blocking of Ad35 vector infection by anti-CD46 antibodies

Next, to further examine which SCR domains in CD46 are used for Ad35 infection, several monoclonal antibodies recognizing

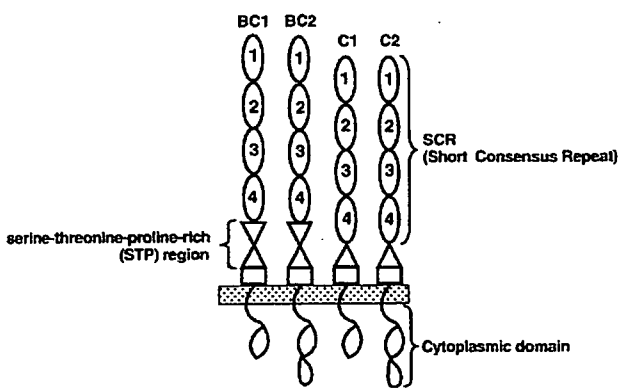

Fig. 1. A schematic diagram of human CD46. Human CD46 is ubiquitously expressed in almost all human cells mainly as four isoforms (BC1, BC2, C1, C2) that are derived via alternative splicing. Human CD46 is composed of four cysteine-rich short consensus repeats (SCRs), a serine–threonine–proline-rich (STP) region, a short region of unknown function, a hydrophobic transmembrane domain, and a carboxy-terminal cytoplasmic domain.

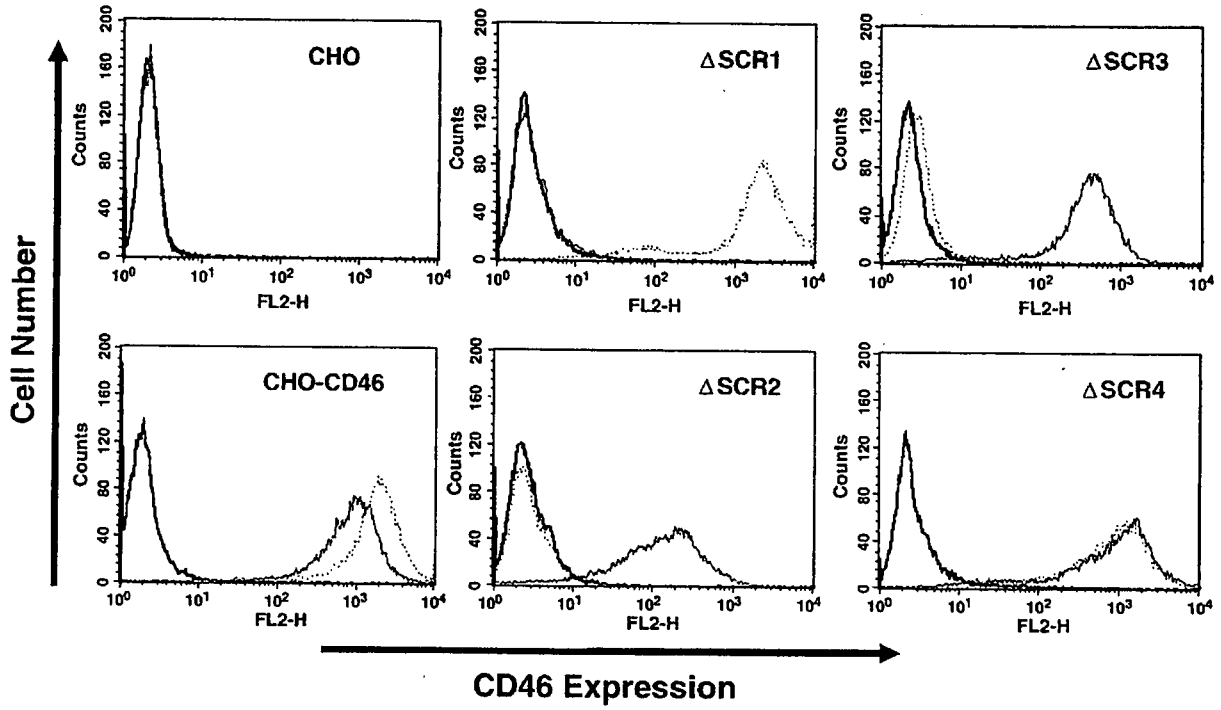

Fig. 2. Expression profiles of CD46 deletion mutants detected by monoclonal anti-CD46 antibodies. The cells were stained with anti-CD46 antibodies against SCR1 (E4.3; thin line), or SCR2 (M177; dotted line), followed by a PE-labeled secondary antibody, and subsequently analyzed by a flowcytometer. ΔSCR3 mutants were treated with anti-CD46 antibody against SCR3 (M160; dotted line) instead of M177. As a negative control, the cells were incubated with irrelevant control IgG, followed by a PE-labeled secondary antibody (thick line).

different domains of CD46 were used to block the transduction with Ad35 vectors. As shown in Fig. 5, the SCR1-specific antibody MEM-258 and the SCR2-specific antibody M177 efficiently inhibited the Ad35 vector-mediated transduction in CHO-CD46 cells. The manufacturer's information indicates that MEM-258 recognizes the SCR4 domain; however, our data indicates that MEM-258 binds to the SCR1 domain (data not shown). A recent study also reported that the epitope of MEM-258 is located in SCR1 [25]. We found that the luciferase production in the presence of both MEM-258 and M177 at 0.5 μg/ml was significantly reduced, compared with each of these antibodies alone (Fig. 5B). In contrast, the antibodies E4.3 and J4-48, which also recognize SCR1, did not decrease the luciferase production by Ad35L, suggesting that the region recognized by MEM-258, but not E4.3 and J4-48, would be involved with Ad35 infection. Decrease in the transduction efficiencies with Ad35L was not also found in the presence of the SCR3-specific antibody M160. The anti-CD46 antibodies which reduced the Ad35 vector-mediated transduction also inhibited the uptake of Ad35L by CHO-CD46 cells in a dose-dependent manner (Fig. 6). The SCR1-specific antibody MEM-258 and

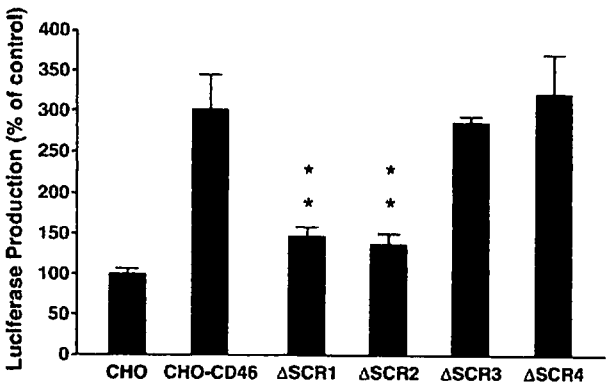

Fig. 3. Ad35L-mediated transduction in CHO cells expressing CD46 mutants lacking SCRs. The cells were transduced with Ad35L at 3000 VP/cell for 1.5 h. The luciferase productions in the cells were measured 48 h after transduction by luminescent assay. The data were normalized to the luciferase production in parental CHO cells. The absolute luciferase production in parental CHO cells was 200 pg/well. The data are expressed as the mean±S.D. (n=4). The asterisks indicate the level of significance (P<0.005 [double asterisk] for comparison with CHO-CD46 cells).

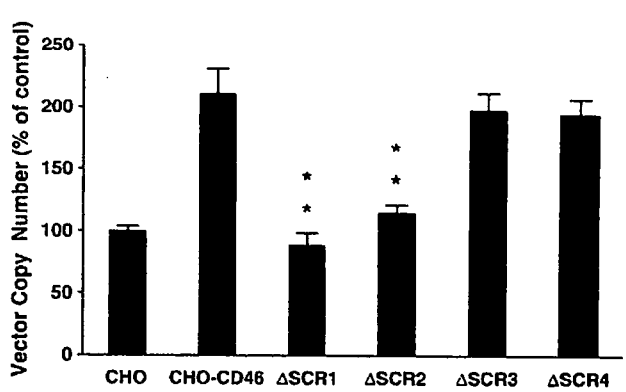

Fig. 4. Cellular uptake of Ad35L in CHO cells expressing CD46 mutants lacking SCRs. The cells were transduced with Ad35L at 3000 VP/cell for 1.5 h. The total DNA, including the vector DNA, was extracted from the cells 48 h after transduction. The copy numbers of the vector DNA were quantified by TaqMan-PCR. The data were normalized to the amounts of the vector DNA in CHO cells. The data are expressed as the mean±S.D. (n=3). The asterisks indicate the level of significance (P<0.005 [double asterisk] for comparison with CHO-CD46 cells).

the SCR2-specific antibody M177 at 5 μg/ml decreased the cellular uptake of Ad35L by 94%. These results suggest that CD46 SCR1 and SCR2 are crucial domains for Ad35 infection.

3.3. Ad35 vector-mediated transduction on CHO cells expressing mutant CD46 lacking the cytoplasmic domain

To examine whether the intracellular domain of human CD46 is required for Ad35 infection, CHO transformants expressing human CD46 C2 isoforms lacking the cytoplasmic domain, CD46ΔCYT0 and CD46ΔCYT6, were transduced with Ad35L. All of the cytoplasmic domain is deleted in CD46ΔCYT0 (amino acid residues 347–369), while CD46ΔCYT6 contains the membrane-proximal 6 amino acids of the cytoplasmic tail and lacks a portion of the cytoplasmic domain (amino acid residues 352–369)

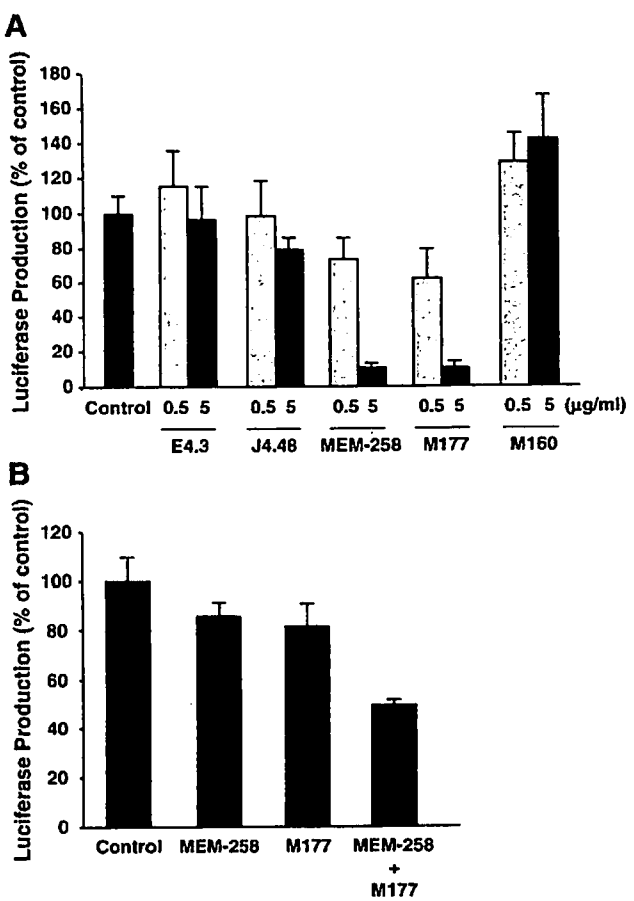

Fig. 5. Blocking of Ad35L-mediated transduction by monoclonal anti-CD46 antibodies. (A) Inhibition of Ad35L-mediated transduction by monoclonal anti-CD46 antibodies. E4.3, MEM-258, and J4-48 (recognizing SCR1), M177 (recognizing SCR2), and M160 (recognizing SCR3) were used as monoclonal anti-CD46 antibodies. CHO cells expressing wild-type CD46 were preincubated with each antibody at the indicated concentrations for 1 h and then infected with Ad35L at 3000 VP/cell. The luciferase productions in the cells were measured by luminescent assay 48 h after transduction. In control settings (Control), the cells were preincubated with medium only prior to transduction. The level of the luciferase production in control settings was almost the same as that in the presence of control mouse IgG (data not shown). (B) Combined inhibitory effect of MEM-258 and M177. The cells were preincubated with MEM-258 and/or M177 at 0.5 μg/ml. The transduction experiments were performed as described above. The data are expressed as the mean±S.D. (n=4).

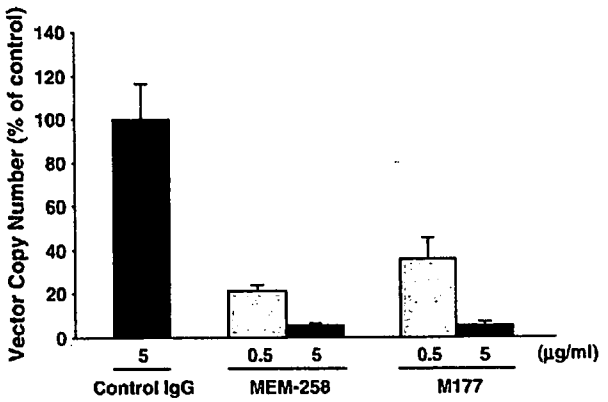

Fig. 6. Inhibition of cellular uptake of Ad35L by monoclonal anti-CD46 antibodies. CHO transformants expressing full-length CD46 were transduced with Ad35L in the presence of anti-CD46 antibody MEM-258 and M177 as described in Fig. 5. The total DNA, including the vector DNA, was extracted 48 h after transduction. The vector copy number was quantified by TaqMan-PCR. The data were normalized to the amounts of the vector DNA in CHO cells expressing full-length CD46 in the presence of control mouse IgG. The data are expressed as the mean±S.D. (n=4).

including the potential phosphorylation domain [26,27], which might be involved with various intracellular events, such as Ca^{2+} flux. The efficiency of the Ad35L-mediated transduction was similar between CHO cells expressing CD46ΔCYT6 and CHO cells expressing the full-length CD46 (Fig. 7). Furthermore, deletion of all the cytoplasmic domain significantly increased the transduction efficiency with Ad35L. These results indicate that the cytoplasmic domain of human CD46 would not be required to serve as a receptor for Ad35.

Next, we further measured the levels of CD46 expression in CHO transformants expressing wild-type CD46 or CD46ΔCYT0 following transduction with Ad35L to investigate why deletion of all the cytoplasmic domain increased the Ad35 vector-mediated transduction efficiency. The cytoplasmic domain is largely responsible to the downregulation of CD46 induced by MV [28], and

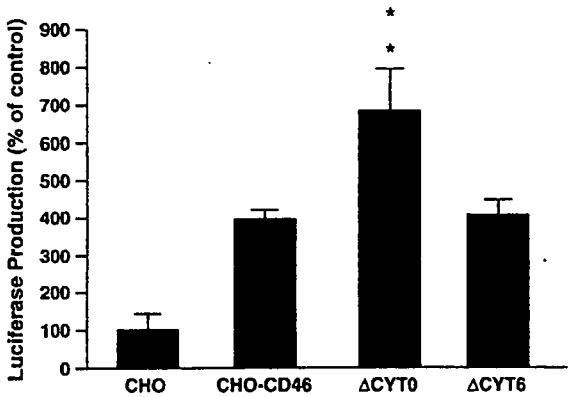

Fig. 7. Ad35L-mediated transduction in CHO cells expressing CD46 mutants lacking the cytoplasmic domain. The cells were transduced with Ad35L at 3000 VP/cells for 1.5 h. The luciferase productions in the cells were measured 48 h after transduction by luminescent assay. The data were normalized to the luciferase production in parental CHO cells. The data are expressed as the mean±S.D. (n=4). The asterisks indicate the level of significance (P<0.005 [double asterisk] for comparison with CHO-CD46).

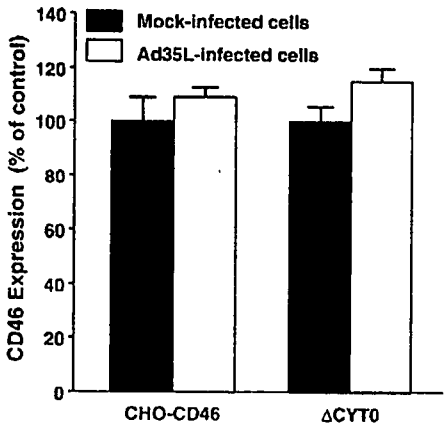

Fig. 8. CD46 expression levels in CHO transformants after infection with Ad35L. The CHO transfonnants expressing full-length CD46 or CD46ΔCYT0 were transduced with Ad35L at 3000 VP/cell for 1.5 h. After a 1.5-h incubation, the cells were subjected to flowcytometric analysis for measurement of CD46 expression. The data are expressed as the mean±S.D. (n=4).

CD46 downregulation might influence the infectivity of the viruses. Flowcytometric analysis demonstrated that CD46 downregulation did not occur in both CHO transfonnants expressing full-length CD46 or CD46ΔCYT0 following transduction with Ad35L (Fig. 8), suggesting that CD46 downregulation by Ad35 vectors was not involved in the increase in the transduction efficiencies of Ad35L in CHO cells expressing CD46ΔCYT0.

4. Discussion

Elucidation of the interaction between viruses and their receptors is of great importance for studies of virus pathogenicity. In addition, for the viruses that provide a framework for gene delivery vehicles, such information may help us not only to evaluate the transduction properties of virus vectors but also to improve virus vectors. In this study, CHO cells expressing CD46 deletion mutants and several monoclonal anti-CD46 antibodies were used to examine which regions are crucial for Ad35 infection. Infection experiments in cells expressing CD46 mutants lacking SCRs and blocking experiments using monoclonal anti-CD46 antibodies have already been used to determine the essential regions for infection of the pathogens recognizing CD46 in previous studies [16–18,29]. We applied this approach to elucidation of the crucial regions in CD46 for subgroup B Ad infection. The results presented herein demonstrated that the essential domains for Ad35 infection are located in SCR1 and 2, and that deletion of all the cytoplasmic domain in CD46 significantly increases Ad35 vector-mediated transduction.

Previous studies have demonstrated that MV binds to SCR1 and 2 [16,17], whereas infection of HHV6 is mediated by SCR2 and 3 [18]. Thus, SCR2 of CD46 is a crucial domain for all the human viruses utilizing CD46 (MV, HHV6, and subgroup B Ads). Moreover, SCR2-specific antibody M177 significantly inhibits the infection of all three viruses (Fig. 3) [18], suggesting that these viruses would interact with the region recognized by M177. The amino acids important for M177 binding, R69 and D70, which are located in the middle of SCR2 [30], are also present in CD46 of the cynomolgus monkey [31], which is susceptible to MV and HHV6. We also confirmed that primary cells isolated from the cynomolgus monkey were efficiently transduced with Ad35 vectors (data not shown).

Deletion of SCR1 as well as SCR2 largely decreased both the transduction efficiency and the cellular uptake of Ad35L (Figs. 3 and 4). However, SCR1-specific E4.3 and J4-48 did not significantly reduce the luciferase productions by Ad35L (Fig. 5). On the other hand, the antibody MEM-258, which also recognizes SCR1, significantly inhibited the Ad35 vector-mediated transduction and cellular uptake of Ad35L (Figs. 5 and 6). The amino acids important for binding of E4.3 and J4-48 are located on the top of SCR1 [31]. At present, it remains unclear where the epitope of MEM-258 is located within SCR1; however, the location of the epitope of MEM-258 would be different from those of E4.3 and J4-48, and would be important for Ad35 infection.

Recognition of SCR1 and 2 by Ad35 would be favorable for infection of Ad35. SCR1 and 2 are located on the upper region of CD46, leading to the decrease in electrostatic repulsion between the virus capsid and acidic cell surface proteins and the increase in attachment of Ad35 to the cell surface. Shayakhmetov and Lieber demonstrated that electrostatic repulsion between the virus capsid and cell surface is an important factor for Ad infection, especially for Ads possessing a short fiber shaft [32]. Ad35 has a shorter fiber shaft (9 nm) than Ad5 (37 nm).

During the preparation of this manuscript, two reports concerning the domains of human CD46 which interact with subgroup B Ads were published [25,33]. Gaggar et al. demonstrated that the subgroup B Ad-binding domain is located within SCR2 alone [33], while Fleischli et al. reported that the presence of both SCR1 and 2 is sufficient for infection of Ad35 and that binding of Ad35 is not confined to a single SCR domain [25]. Our data support the conclusion of Fleischli et al. The SCR2-specific antibody M177 and the deletion of SCR2 decreased Ad35 vector-mediated transduction (Figs. 3–6), suggesting that the region in SCR2 recognized by M177 would be important for interaction with Ad35. Luciferase production by Ad35L and cellular uptake of Ad35L in ΔSCR1 mutants was largely decreased, compared with CHO-CD46 cells (Figs. 3 and 4), suggesting that SCR1 would also play a role in Ad35 infection. Although the decrease in luciferase production and cellular uptake of Ad35L in the ΔSCR1 mutant might be due to conformational change of SCR2 by the deletion of SCR1, this is unlikely because the SCR2-specific antibody M177 showed positive staining in the ΔSCR1 mutant (Fig. 2). This suggests that the region recognized by M177 would hold an appropriate conformation in the ΔSCR1 mutant. Therefore, we conclude that both SCR1 and SCR2 are involved with Ad35 infection. The finding that the SCR1-specific antibody MEM-258 largely inhibited the transduction with Ad35L supports this conclusion (Figs. 5 and 6).

The cytoplasmic domain of human CD46 is not an absolute requirement in order for this protein to serve as an attachment receptor for Ad35 (Fig. 7). MV and HHV6 can also infect cells via mutant CD46 lacking the cytoplasmic domain [18,19]. However, the luciferase production was significantly increased in ΔCYT0, compared with that in CHO-CD46, in contrast, Ad35L mediated similar levels of luciferase productions in both CHO-CD46 and ΔCYT6. It remains unclear why the deletion of

the entire cytoplasmic domain of human CD46 increased the transduction efficiency, however, downregulation of CD46 was not observed in both CHO-CD46 and ΔCYT0 after transduction with Ad35L (Fig. 7). These results suggest that the increase in the transduction efficiencies of Ad35L in ΔCYT0 was not due to the lack of CD46 downregulation. One possibility for the increased transduction efficiencies in ΔCYT0 is that the amounts of CD46 which Ad35 vectors can access to would be increased by the deletion of the cytoplasmic domain. Maisner et al. demonstrated that CD46 are predominantly distributed in basolateral side of the cells and that CD46 lacking the entire cytoplasmic domain were transported to both apical and basolateral sides [34]. CD46ΔCYT0 might be more widely distributed than full-length CD46 in the CHO transformants, leading to the increase in the infection of Ad35 vectors. Another possibility is that the membrane-proximal 6 amino acids of the cytoplasmic domain in CD46 C2 isoform might contain a signal sequence for suppression of viral infection. Mouse macrophages expressing a tailless human CD46 mutant are more susceptible to MV infection than those expressing wild-type CD46 [35]. In addition to these functions of the cytoplasmic domain, the cytoplasmic domain plays important roles in immune responses through CD46, such as cytokine productions. Hirano et al. reported that the production of high levels of NO and IL-12 upon MV infection is dependent on the CD46 cytoplasmic domain [35]. Kurita-Taniguchi et al. demonstrated that intracellular phosphatase SHP-1 was found to be recruited to the cytoplasmic tail of human CD46 when human macrophages became sufficiently mature to produce IL-12 and NO in response to measles virus [36]. Therefore, the cytoplasmic domain might be involved with immune responses induced by Ad35 infection.

In summary, we demonstrated here that SCR1 and 2 of human CD46 are required for Ad35 infection, while the cytoplasmic domain of human CD46 is not crucial for an attachment receptor function for Ad35. These results offer insight into the interaction between human CD46 and subgroup B Ads, such as the internalization of Ad35 into the cells via CD46 and the crucial domain in the Ad35 fiber knob for binding to CD46.

Acknowledgements

We would like to thank Dr. Yasuko Mori (Laboratory of Virology and Vaccinology, National Institute of Biomedical Innovation, Osaka, Japan) for her advice on the cell culture. This work was supported in part by a Grants-in-Aid for Scientific Research from the Ministry of Education, Culture, Sports, Science, and Technology of Japan, and by grants for Health and Labour Sciences Research from the Ministry of Health, Labour, and Welfare of Japan.

References

[1] M.J. Havenga, A.A. Lemckert, O.J. Ophorst, M. van Meijer, W.T. Germenad, J. Grimbergen, M.A. van Den Doel, R. Vogels, J. van Deutekom, A.A. Janson, J.D. de Bruijn, F. Uytdehaag, P.H. Quax, T. Logtenberg, M. Mehtali, A. Bout, Exploiting the natural diversity in adenovirus tropism for therapy and prevention of disease, J. Virol. 76 (2002) 4612–4620.

[2] J.C. De Jong, A.G. Wermenbol, M.W. Verweij-Uijterwaal, K.W. Slaterus, P. Wertheim-Van Dillen, G.J. Van Doornum, S.H. Khoo, J.C. Hierholzer, Adenoviruses from human immunodeficiency virus-infected individuals, including two strains that represent new candidate serotypes Ad50 and Ad51 of species B1 and D, respectively, J. Clin. Microbiol. 37 (1999) 3940–3945.

[3] R. Vogels, D. Zuijdgeest, R. van Rijnsoever, E. Hartkoorn, I. Damen, M.P. de Bethune, S. Kostense, G. Penders, N. Helmus, W. Koudstaal, M. Cecchini, A. Wetterwald, M. Sprangers, A. Lemckert, O. Ophorst, B. Koel, M. van Meerendonk, P. Quax, L. Panitti, J. Grimbergen, A. Bout, J. Goudsmit, M. Havenga, Replication-deficient human adenovirus type 35 vectors for gene transfer and vaccination: efficient human cell infection and bypass of preexisting adenovirus immunity, J. Virol. 77 (2003) 8263–8271.

[4] A. Gaggar, D.M. Shayakhmetov, A. Lieber, CD46 is a cellular receptor for group B adenoviruses, Nat. Med. 9 (2003) 1408–1412.

[5] A. Segerman, J.P. Atkinson, M. Marttila, V. Dennerquist, G. Wadell, N. Arnberg, Adenovirus type 11 uses CD46 as a cellular receptor, J. Virol. 77 (2003) 9183–9191.

[6] F. Sakurai, H. Mizuguchi, T. Hayakawa, Efficient gene transfer into human CD34+ cells by an adenovirus type 35 vector, Gene Ther. 10 (2003) 1041–1048.

[7] F. Sakurai, H. Mizuguchi, T. Yamaguchi, T. Hayakawa, Characterization of in vitro and in vivo gene transfer properties of adenovirus serotype 35 vector, Mol. Ther. 8 (2003) 813–821.

[8] T. Seya, J.R. Turner, J.P. Atkinson, Purification and characterization of a membrane protein (gp45-70) that is a cofactor for cleavage of C3b and C4b, J. Exp. Med. 163 (1986) 837–855.

[9] T. Seya, J.P. Atkinson, Functional properties of membrane cofactor protein of complement, Biochem. J. 264 (1989) 581–588.

[10] T. Seya, T. Hara, M. Matsumoto, Y. Sugita, H. Akedo, Complement-mediated tumor cell damage induced by antibodies against membrane cofactor protein (MCP, CD46), J. Exp. Med. 172 (1990) 1673–1680.

[11] D.M. Lublin, K.E. Coyne, Phospholipid-anchored and transmembrane versions of either decay-accelerating factor or membrane cofactor protein show equal efficiency in protection from complement-mediated cell damage, J. Exp. Med. 174 (1991) 35–44.

[12] F. Santoro, P.E. Kennedy, G. Locatelli, M.S. Malnati, E.A. Berger, P. Lusso, CD46 is a cellular receptor for human herpesvirus 6, Cell 99 (1999) 817–827.

[13] R.E. Dorig, A. Marcil, A. Chopra, C.D. Richardson, The human CD46 molecule is a receptor for measles virus (Edmonston strain), Cell 75 (1993) 295–305.

[14] H. Kallstrom, M.K. Liszewski, J.P. Atkinson, A.B. Jonsson, Membrane cofactor protein (MCP or CD46) is a cellular pilus receptor for pathogenic *Neisseria*, Mol. Microbiol. 25 (1997) 639–647.

[15] N. Okada, M.K. Liszewski, J.P. Atkinson, M. Caparon, Membrane cofactor protein (CD46) is a keratinocyte receptor for the M protein of the group A streptococcus, Proc. Natl. Acad. Sci. U. S. A. 92 (1995) 2489–2493.

[16] K. Iwata, T. Seya, Y. Yanagi, J.M. Pesando, P.M. Johnson, M. Okabe, S. Ueda, H. Ariga, S. Nagasawa, Diversity of sites for measles virus binding and for inactivation of complement C3b and C4b on membrane cofactor protein CD46, J. Biol. Chem. 270 (1995) 15148–15152.

[17] M. Manchester, A. Valsamakis, R. Kaufman, M.K. Liszewski, J. Alvarez, J.P. Atkinson, D.M. Lublin, M.B. Oldstone, Measles virus and C3 binding sites are distinct on membrane cofactor protein (CD46), Proc. Natl. Acad. Sci. U. S. A. 92 (1995) 2303–2307.

[18] H.L. Greenstone, F. Santoro, P. Lusso, E.A. Berger, Human herpesvirus 6 and measles virus employ distinct CD46 domains for receptor function, J. Biol. Chem. 277 (2002) 39112–39118.

[19] T. Seya, M. Kurita, K. Iwata, Y. Yanagi, K. Tanaka, K. Shida, M. Hatanaka, M. Matsumoto, S. Jun, A. Hirano, S. Ueda, S. Nagasawa, The CD46 transmembrane domain is required for efficient formation of measles-virus-mediated syncytium, Biochem. J. 322 (Pt 1) (1997) 135–144.

[20] T. Seya, T. Hara, M. Matsumoto, H. Akedo, Quantitative analysis of membrane cofactor protein (MCP) of complement. High expression of MCP on human leukemia cell lines, which is down-regulated during cell differentiation, J. Immunol. 145 (1990) 238–245.

[21] F. Sakurai, K. Kawabata, T. Yamaguchi, T. Hayakawa, H. Mizuguchi, Optimization of adenovirus serotype 35 vectors for efficient transduction in human hematopoietic progenitors: comparison of promoter activities, Gene Ther. 12 (2005) 1424–1433.

[22] H. Mizuguchi, N. Koizumi, T. Hosono, N. Utoguchi, Y. Watanabe, M.A. Kay, T. Hayakawa, A simplified system for constructing recombinant adenoviral vectors containing heterologous peptides in the HI loop of their fiber knob, Gene Ther. 8 (2001) 730–735.
[23] V. Krougliak, F.L. Graham, Development of cell lines capable of complementing E1, E4, and protein IX defective adenovirus type 5 mutants, Hum. Gene Ther. 6 (1995) 1575–1586.
[24] J.V. Maizel Jr., D.O. White, M.D. Scharff, The polypeptides of adenovirus. I. Evidence for multiple protein components in the virion and a comparison of types 2, 7A, and 12, Virology 36 (1968) 115–125.
[25] C. Fleischli, S. Verhaagh, M. Havenga, D. Sirena, W. Schaffner, R. Cattaneo, U.F. Greber, S. Hemmi, The distal short consensus repeats 1 and 2 of the membrane cofactor protein CD46 and their distance from the cell membrane determine productive entry of species B adenovirus serotype 35, J. Virol. 79 (2005) 10013–10022.
[26] M.K. Liszewski, I. Tedja, J.P. Atkinson, Membrane cofactor protein (CD46) of complement. Processing differences related to alternatively spliced cytoplasmic domains, J. Biol. Chem. 269 (1994) 10776–10779.
[27] G. Wang, M.K. Liszewski, A.C. Chan, J.P. Atkinson, Membrane cofactor protein (MCP; CD46): isoform-specific tyrosine phosphorylation, J. Immunol. 164 (2000) 1839–1846.
[28] A. Hirano, S. Yant, K. Iwata, J. Korte-Sarfaty, T. Seya, S. Nagasawa, T.C. Wong, Human cell receptor CD46 is down regulated through recognition of a membrane-proximal region of the cytoplasmic domain in persistent measles virus infection, J. Virol. 70 (1996) 6929–6936.
[29] Y. Mori, T. Seya, H.L. Huang, P. Akkapaiboon, P. Dhepakson, K. Yamanishi, Human herpesvirus 6 variant A but not variant B induces fusion from without in a variety of human cells through a human herpesvirus 6 entry receptor, CD46, J. Virol. 76 (2002) 6750–6761.
[30] C.J. Buchholz, D. Koller, P. Devaux, C. Mumenthaler, J. Schneider-Schaulies, W. Braun, D. Gerlier, R. Cattaneo, Mapping of the primary binding site of measles virus to its receptor CD46, J. Biol. Chem. 272 (1997) 22072–22079.
[31] E.C. Hsu, S. Sabatinos, F.J. Hoedemaeker, D.R. Rose, C.D. Richardson, Use of site-specific mutagenesis and monoclonal antibodies to map regions of CD46 that interact with measles virus H protein, Virology 258 (1999) 314–326.
[32] D.M. Shayakhmetov, A. Lieber, Dependence of adenovirus infectivity on length of the fiber shaft domain, J. Virol. 74 (2000) 10274–10286.
[33] A. Gaggar, D.M. Shayakhmetov, M.K. Liszewski, J.P. Atkinson, A. Lieber, Localization of regions in CD46 that interact with adenovirus, J. Virol. 79 (2005) 7503–7513.
[34] A. Maisner, M.K. Liszewski, J.P. Atkinson, R. Schwartz-Albiez, G. Herrler, Two different cytoplasmic tails direct isoforms of the membrane cofactor protein (CD46) to the basolateral surface of Madin–Darby canine kidney cells, J. Biol. Chem. 271 (1996) 18853–18858.
[35] A. Hirano, Z. Yang, Y. Katayama, J. Korte-Sarfaty, T.C. Wong, Human CD46 enhances nitric oxide production in mouse macrophages in response to measles virus infection in the presence of gamma interferon: dependence on the CD46 cytoplasmic domains, J. Virol. 73 (1999) 4776–4785.
[36] M. Kurita-Taniguchi, A. Fukui, K. Hazeki, A. Hirano, S. Tsuji, M. Matsumoto, M. Watanabe, S. Ueda, T. Seya, Functional modulation of human macrophages through CD46 (measles virus receptor): production of IL-12 p40 and nitric oxide in association with recruitment of protein-tyrosine phosphatase SHP-1 to CD46, J. Immunol. 165 (2000) 5143–5152.

Arteriosclerosis, Thrombosis, and Vascular Biology

JOURNAL OF THE AMERICAN HEART ASSOCIATION

A Central Role for Nicotinic Cholinergic Regulation of Growth Factor–Induced Endothelial Cell Migration

Martin K.C. Ng, Jenny Wu, Edwin Chang, Bing-yin Wang, Regina Katzenberg-Clark, Akiko Ishii-Watabe and John P. Cooke

Arterioscler. Thromb. Vasc. Biol. 2007;27;106-112; originally published online Nov 2, 2006;

DOI: 10.1161/01.ATV.0000251517.98396.4a

Arteriosclerosis, Thrombosis, and Vascular Biology is published by the American Heart Association. 7272 Greenville Avenue, Dallas, TX 72514

 Print ISSN: 1079-5642. Online ISSN: 1524-4636